

Isostructural Series of Nine-Coordinate Chiral Lanthanide Complexes Based on Triazacyclononane

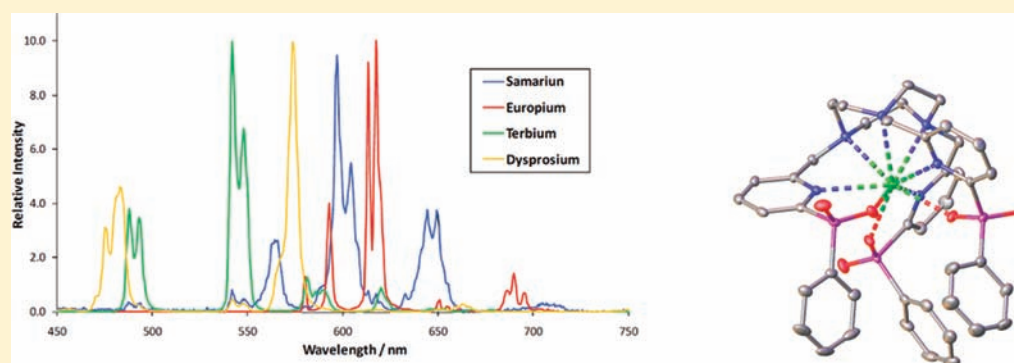
James W. Walton,[†] Rachel Carr,[†] Nicholas H. Evans,[†] Alexander M. Funk,[†] Alan M. Kenwright,[†] David Parker,^{*,†} Dmitry S. Yufit,[†] Mauro Botta,[‡] Sara De Pinto,[‡] and Ka-Leung Wong[§]

[†]Department of Chemistry, Durham University, South Road, Durham DH1 3LE, U.K.

[‡]Dipartimento di Scienze e Innovazione Tecnologica, Università del Piemonte Orientale, "Amedeo Avogadro" Viale Teresa Michel 11, 15121 Alessandria, Italy

[§]Department of Chemistry, Hong Kong Baptist University, Kowloon Tong, Hong Kong

S Supporting Information



ABSTRACT: Nonadentate ligands based on triazacyclononane incorporating pyridyl-2-phosphinate groups form an isostructural series of complexes with Ln ions in the solid state and in solution. The Ln ion is effectively shielded from the solvent environment. Crystal structures reveal a rigid C_3 -symmetric tricapped trigonal-prismatic coordination geometry that is maintained in solution for the methyl and phenylphosphinate series, as shown by multinuclear NMR analysis. Variable-temperature measurements of the field dependence of the water proton relaxivity in gadolinium complexes indicate that these systems exclude solvent from the primary coordination environment and minimize the second sphere of solvation. The electronic relaxation time for the gadolinium methylphosphinate complex has been estimated to be 550 (± 150) ps by EPR and NMR methods, compared to values of around 0.30–0.05 ps for the terbium–ytterbium series, deduced by analyzing the field dependence (4.7–16.5 T) of the ^{31}P NMR longitudinal relaxation times. Values are compared with analogous azacarboxylate ligand complexes, supporting a key role for donor atom polarizability in determining the electronic relaxation. Spectral emission behavior in solution of samarium, europium, terbium, and dysprosium complexes is compared, and the resolved $RRR-\Lambda$ and $SSS-\Delta$ complexes show strong circularly polarized luminescence. The molecular quadratic hyperpolarizability $\langle\beta_{\text{HLS}}\rangle$ has been measured in solution using hyper-Raleigh light-scattering methods, for the whole series of lanthanide complexes of one ligand. The values of $\langle\beta_{\text{HLS}}\rangle$ reach a maximum around the center of the series and are not simply dependent on the number of f electrons, suggesting a dominant contribution from the octupolar rather than the dipolar term.

INTRODUCTION

Nonadentate ligands forming an isostructural series of complexes with Ln^{III} ions are not common, compared to the very large number of octadentate ligands forming well-defined 1:1 complexes. The identification of such an isostructural series allows various comparative physicochemical studies to be undertaken, examining behavior across the series.

In this work, the first set of studies relates to applications in photo- and electroluminescence, where stability with respect to deactivation of the long-lived lanthanide excited state is sought, typically by shielding the coordinated ion from intermolecular quenching processes, such as vibrational deactivation by the solvent.¹ This aspect is a key, underpinning requirement in the

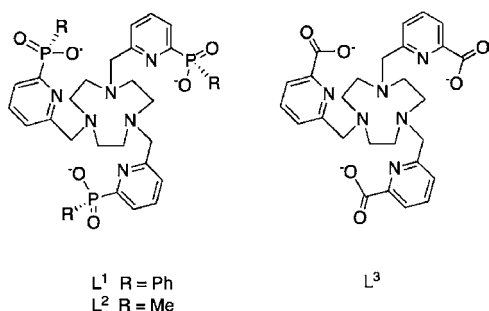
development of new emissive tags for labeling purposes, allowing their exploitation in time-resolved bioassays, for example. These systems are also of interest as purely “outer-sphere” magnetic resonance (MR) probes for macromolecular structural analysis, taking advantage of the high paramagnetism of the central Ln^{III} ions. Such nonadentate ligands may have C_3 symmetry, allowing a comparison of their spectral properties to be made with “classical” ML_3 complexes of certain tridentate ligands, such as oxydiacetate and dipicolinate (pyridine-2,6-dicarboxylate) and their analogues and derivatives.²

Received: January 19, 2012

Published: July 19, 2012

A convenient platform for their preparation uses 1,4,7-triazacyclononane, which occupies three sites in a tricapped trigonal-prismatic coordination geometry. This approach has been reported previously, notably by Ziessel, Mazzanti, and Tei,³ examining azacarboxylate examples. A set of iminoazaphosphonate complexes has also been structurally characterized, but the lanthanide complexes were prone to both ester and imine hydrolysis in aqueous solution,^{3c} leading to metal-ion dissociation. Here, we report the structure and properties of the neutral lanthanide(III) complexes of ligands L^1 and L^2 , containing P–Ph and P–Me substituents, respectively (Chart 1), where the P substituent was envisaged to create steric bulk

Chart 1. Structures of Ligands L^1 – L^3



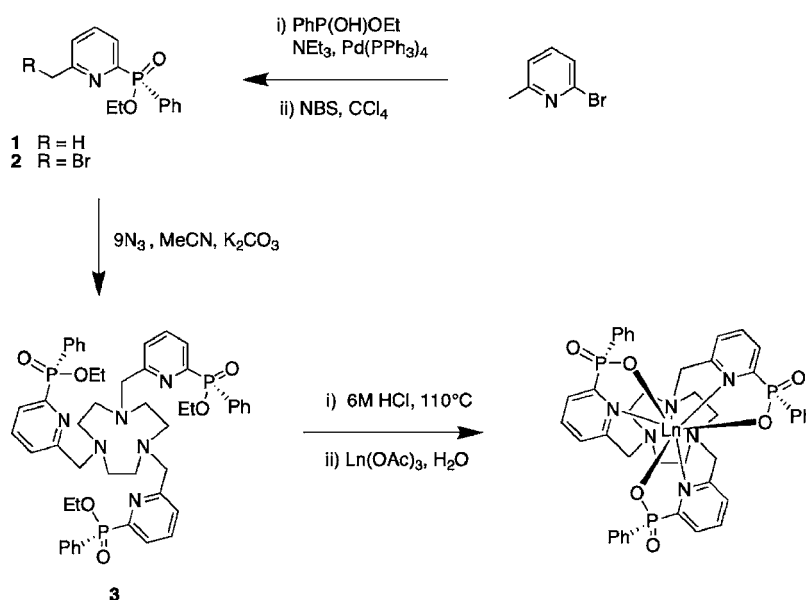
opposite the macrocyclic ring, effectively shielding the Ln ion from the environment. A comparison is made with the properties of the less bulky carboxylate complex analogues, based on L^3 .^{3b,c}

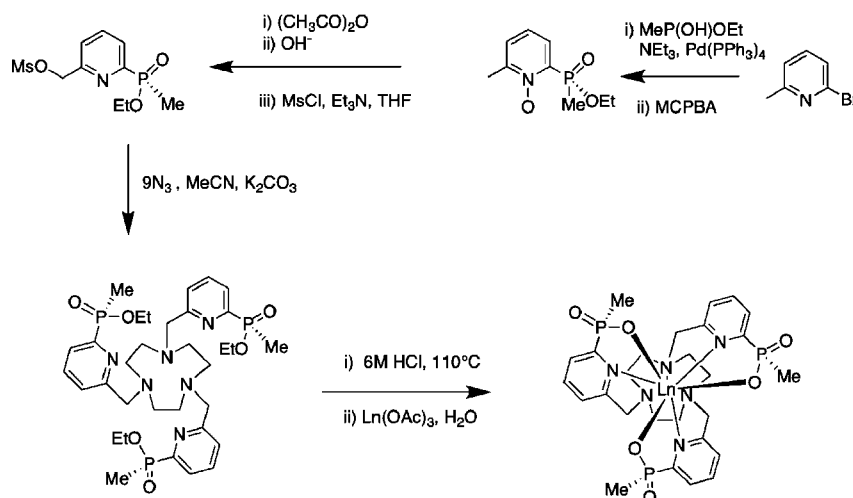
Complexes of d-block, rare-earth, and group 13 metal ions with phosphinate analogues of azacarboxylate ligands have been explored over the past 20 years.^{4,5} The pentavalency of phosphorus allows control over ligand lipophilicity and also offers a point of conjugation. In addition, metal coordination gives rise to a tetrahedral, stereogenic center at phosphorus, facilitating the separation of chiral complexes that are resistant to racemization.^{4b}

The crystallographic analysis of seven lanthanide complexes of L^1 is reported, allowing the definition of an isostructural series in the solid state. A preliminary communication has been published, focusing on the structural and chiroptical properties of complexes of L^1 .⁶ Here, solution-state NMR properties of the complexes are assessed in detail and the relaxation effects of the purely “outer-sphere” gadolinium(III) complexes in aqueous solution examined, using variable-temperature (VT) and variable-field (VF) ^1H NMR measurements. This allows additional information to be gained on the electronic relaxation time of gadolinium, allowing the effect of donor atom perturbation in a common symmetry to be studied. Examination of the field dependence (4.7–16.5 T) of the intramolecular longitudinal relaxation rate of the ^{31}P nucleus by the proximate Ln ion has also been undertaken, allowing an estimate of Ln ion electronic relaxation times for Tb, Dy, Ho, Er, Tm, and Yb to be made, using global fitting methods. There is no consensus in the literature about the factors that determine lanthanide electronic relaxation rates in solution. Suggestions have been made of links to the local metal-ion symmetry and overall complex rigidity, but there are very few rigorous and comparative studies that examine complexes that belong to an isostructural series.

Furthermore, the molecular quadratic hyperpolarizability (β_{HLS}) of the complexes (yttrium and cerium to ytterbium) has been measured in a methanol solution, using harmonic light-scattering techniques. This allows a direct comparison with recent work with C_3 -symmetric tris(picolate) complexes, such as $[\text{Ln}(\text{dpa})_3]$ (dpa = pyridine-2,6-dicarboxylate).⁷ The nonlinear optical properties of lanthanide(III) complexes have been the subject of some controversy recently; notably, the relative importance of the number of f electrons in determining either the dipolar or octupolar contributions to the measured quadratic hyperpolarizability has been the subject of debate.^{8–10} The work presented here allows a comparison with published data to be made, enabling further information to be gained on the correlation between the ligand structure and hyperpolarizability. Obviously, such analysis can only be undertaken

Scheme 1. Synthesis of Lanthanide Complexes of L^1



Scheme 2. Synthesis of Lanthanide Complexes of L^2 

with confidence because of the isostructural nature of this series.

RESULTS AND DISCUSSION

Ligand Synthesis and Complex Characterization. The syntheses of ligands H_3L^1 and H_3L^2 followed slightly different routes, culminating in alkylation of triazacyclononane in an acetonitrile solution. The reaction of 2-bromo-6-methylpyridine with PhP(OH)OEt under palladium catalysis allowed formation of the C–P bond to give the phosphinate ester **1** (Scheme 1). Subsequent selective allylic bromination (*N*-bromosuccinimide and CCl_4) yielded the 6-bromomethyl derivative **2**, which was reacted with 0.33 equiv of triazacyclononane to afford the triester **3** as a major diastereoisomer. Acid hydrolysis followed by complexation with the appropriate Ln(OAc)_3 or LnCl_3 salt yielded the neutral lanthanide(III) complexes.⁶ These complexes were purified by chromatography on a short silica column, and their purity was assessed by elemental analysis. Each complex gave rise to a single species, as deduced by reverse-phase high-performance liquid chromatography (HPLC), consistent with the presence of a single diastereoisomer.

For the synthesis of the *PMe* analogue, L^2 , functionalization of the 6-Me group was undertaken in a different manner (Scheme 2). The reaction of the intermediate pyridylmethylphosphinate ester with *m*CPBA followed by treatment with acetic anhydride afforded the labile acetate ester via a Boekelheide rearrangement.¹¹ Following ester hydrolysis, the mesylate was formed in high yield and used to alkylate triazacyclononane in an $\text{S}_{\text{N}}2$ reaction. The mesylate proved to be less reactive than the corresponding benzylic bromide and gave significantly less of the tetra-*N*-alkylated product. This aspect was assessed by analysis of the crude reaction mixtures using electrospray mass spectrometry (ESMS).

The lanthanide complexes of L^1 were sparingly soluble in water but dissolved readily in methanol. Simple tests of solubility (using molar extinction coefficients to calibrate) revealed that the europium complex of L^2 was about 60 times more soluble in water than the complex of L^1 , in accordance with the change from a phenyl group to a less hydrophobic methyl substituent.

Crystals of $[\text{Ln}L^1]$ grew readily over a period of a few hours from aqueous methanol (1:2). The structures of six complexes

(neodymium, samarium, europium, holmium, thulium, and ytterbium) were reported earlier⁶ and contained varying amounts of disordered water molecules. Each complex formed monoclinic crystals in the space group $P2_1/n$, defining an isostructural series. The cerium analogue is reported here and crystallized in two forms in different space groups (see the Experimental Section). The first to form crystallized in a triclinic space group ($P\bar{1}$; Table 1) and slowly converted to a

Table 1. Crystallographic Data for $[\text{Ce}L^1]$

empirical formula	$\text{C}_{42}\text{H}_{42}\text{N}_6\text{O}_6\text{P}_3\text{Ce}$
fw	959.85
temperature/K	120
cryst syst	triclinic
space group	$P\bar{1}$
<i>a</i> /Å	11.2660(2)
<i>b</i> /Å	14.0690(4)
<i>c</i> /Å	17.2816(3)
α /deg	110.4195(19)
β /deg	99.5765(17)
γ /deg	101.542(2)
volume/Å ³	2430.50(9)
<i>Z</i>	2
reflns collected	40 084
indep reflns	13 519 [$R(\text{int}) = 0.0545$]
GOF on F^2	0.981
final <i>R</i> indexes [$I \geq 2\sigma(I)$]	$R_1 = 0.0366$, $wR_2 = 0.0801$
final <i>R</i> indexes [all data]	$R_1 = 0.0473$, $wR_2 = 0.0837$

more hydrated monoclinic form over several days. In each case, the same molecular structure was apparent.

The Ce ion is coordinated by the three N atoms of the 1,4,7-triazacyclononane ring and each pyridyl N and phosphinate O atom (Figure 1). The coordination geometry is a distorted tricapped trigonal prism, with a pseudo- C_3 axis passing through the center of the nine-membered triazacyclononane ring. Only the *RRR* and *SSS* complexes were present in the unit cell. For an *R* configuration at P, the ring *NCCN* and substituent *NCCN_{py}* torsion angles averaged $+47^\circ$ and -33° . This behavior is consistent with a $\delta\delta\delta$ chelate ring conformation and a complex Λ configuration. For $[\text{Ln}L^1]$, after allowing for ionic radius variation, the Ln–N bonds were almost identical with those found for the related carboxylate series $[\text{Ln}L^3]$ (Ln = Gd,

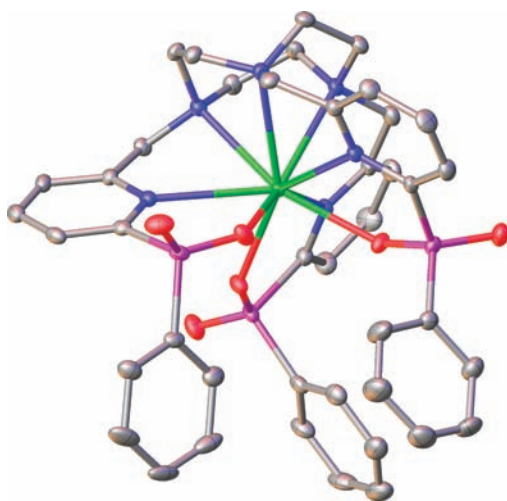


Figure 1. View of the molecular structure of RRR- Λ -[CeL¹] (120 K).

Tb, Lu)^{3b} but with a shorter Ln–O bond and a longer bond to each pyridyl N atom. Bond-length values for the lanthanide(III) complexes followed the expected contraction in the ionic radius¹² (Table 2), with the Ln ion size reduction being

Table 2. Selected Mean Distances of Ligand Atoms to the Ln Ion^a (Å, ± 0.02) for [LnL¹]

Ln ^{II}	Ce	Nd	Sm	Eu	Ho	Tm	Yb
Ln–O	2.41	2.37	2.34	2.33	2.29	2.26	2.25
Ln–N	2.75	2.71	2.69	2.68	2.65	2.63	2.62
Ln–N _{py}	2.73	2.69	2.67	2.66	2.63	2.62	2.62
Ln–P	3.62	3.58	3.55	3.54	3.51	3.49	3.48

^aEffective ionic radii (Å) in nine-coordinate systems¹² are as follows: Ce (1.20); Nd (1.16); Sm (1.13); Eu (1.12); Ho (1.07); Tm (1.05); Yb (1.04).

reflected monotonously by a decrease in the Ln–O distance. The selective formation of metal complex diastereoisomers with the same configuration at P has previously been observed in C₄-symmetric lanthanide complexes based on cyclen tetraphosphinates^{4a,13} and in octahedral complexes of iron, cobalt, nickel, copper, zinc, and gallium with a hexadentate tris-(phenylphosphinate) ligand based on triazacyclononane.^{5b}

Solution NMR Analysis. For the yttrium and lanthanide complexes of L¹, one ³¹P NMR resonance and 12 distinct ¹H NMR resonances were observed, consistent with the presence of one C₃-symmetric species in a methanol-*d*₄ solution at 295 K. With [YL¹], analysis of the COSY spectrum allows each proton to be assigned (Figure 2). In the aromatic region, the meta, para, and ortho protons of the phenyl ring are readily assigned, with the ortho protons resonating to highest frequency because of the shielding effect of the P–O double bond. The *o*-phenyl proton resonance overlapped with that due to H⁴ on the pyridine ring, and H³ and H⁵ were distinguished by the presence of a ³J coupling between H³ and P of 10 Hz.

The diastereotopic pyridyl methylene protons were anisochronous and resonated as a first-order AB multiplet with $\Delta\delta$ of 0.85 ppm and a ²J value of –16 Hz. Within each of the macrocyclic NCCN chelate rings, the axial and equatorial protons defined an AA'BB' multiplet. The axial protons are readily distinguished because they possess a very large geminal coupling constant to the equatorial proton and a large vicinal coupling constant (ca. 8.5 Hz) to the antiperiplanar axial

proton, creating the appearance of a broadened triplet. Hence, one axial proton resonates at 3.62 ppm (Figure 2), and the geminal equatorial proton resonates as a broadened doublet at 2.86 ppm. The other pair of axial and equatorial protons is nearly isochronous, resonating at 2.65 ppm. In the related carboxylate complex [YL³], the pyridyl methylene groups resonated only 0.02 ppm apart (14.1 T, 295 K, D₂O), centered around 4.12 ppm, while the ring methylene protons resonated at 3.59 (H_{ax}), 2.90 (H_{eq}), 2.63 (H_{eq}), and 2.30 ppm (H_{ax}), respectively. In [YL¹], the P–O double bond is not conjugated with the pyridyl π ring and the pro-(*S*)-pyridyl methylene proton is directed toward it (viz. Figure 1) and so resonates to higher frequency (4.95 ppm). This shielding effect rationalizes the chemical shift behavior of the pyridyl methylene protons in the yttrium complexes of L¹ and L³ and allows a complete ¹H NMR spectral assignment. At 323 K, the overall form and appearance of the spectrum showed very little change, suggesting that δ/λ NCCN interconversion (exchanging axial and equatorial positions) and pendant arm rotation (rendering the CH₂py methylene hydrogens equivalent) were slow on the NMR time scale at this temperature.

The ¹H NMR spectra of the europium complexes of L¹, L², and L³ were also assigned (see the Experimental Section and Supporting Information) and showed the presence of one major C₃-symmetric species. Because these three complexes form a closely related series, it was straightforward to assign the phenyl and methyl resonances in [EuL¹] and [EuL²] and the common pyridyl resonances in each case. For the assignment of the remaining methylene protons, both ¹H NMR COSY methods and measurements of the longitudinal relaxation rates, R₁, of each observed resonance (at 4.7 and 9.4 T) were used.¹⁴ In the latter case, the rate of relaxation varies with the distance from the Ln ion as r^{-6} and increases with the field (see below); the closer the proton is to the Ln ion, the faster the rate, R₁. Because the distances of each proton to the Eu ion are known from the X-ray structural analyses, this allowed a full assignment (Experimental Section). For example, the pair of pyCH₂ protons resonated at 7.51 and –0.10 ppm in [EuL¹]; in the former case, the R₁ value (295 K, 4.7 T) was 20 Hz compared to 10 Hz for the other. Thus, the resonance at 7.51 ppm must lie closer to the Eu ion and can be assigned to be the pro-*S* hydrogen in the Λ -RRR complex; an inspection of the X-ray structure of [EuL¹] shows that the pro-*S* hydrogen is 3.50 Å from the Eu ion, compared to 4.35 Å for the pro-*R* hydrogen. A partial assignment for [EuL³] was published earlier,^{3b} and the results reported here are in reasonable agreement, although the cited ¹H-coupled multiplets were not observed, either at 4.7 or 9.4 T. The chemical shift values of the ring protons were very similar for each of these europium complexes, suggesting that the second-order crystal-field coefficient, B²₀, which is directly proportional to the magnitude of the pseudocontact shift in the classical Bleaney analysis, is similar in each case.¹⁵ Given the very similar dipolar coordinates for the ring protons in these isostructural series, this behavior is consistent with a dominant contribution to this ligand-field term from the common N donors, rather than the anionic O atoms.

The ¹H and ¹³C NMR spectra of [YbL¹] were also examined in CD₃OD at 295 and 323 K (Figure 3). In the latter case, three methylene resonances were evident, with the benzylic C atoms at 71.2 ppm and the macrocyclic ring methylene C atoms at 46.8 and 36.3. At 323 K, the ring C atoms were separated by 9.1 ppm and showed no evidence of exchange broadening. The overall form of the ¹H NMR spectra of [YbL¹] also did not

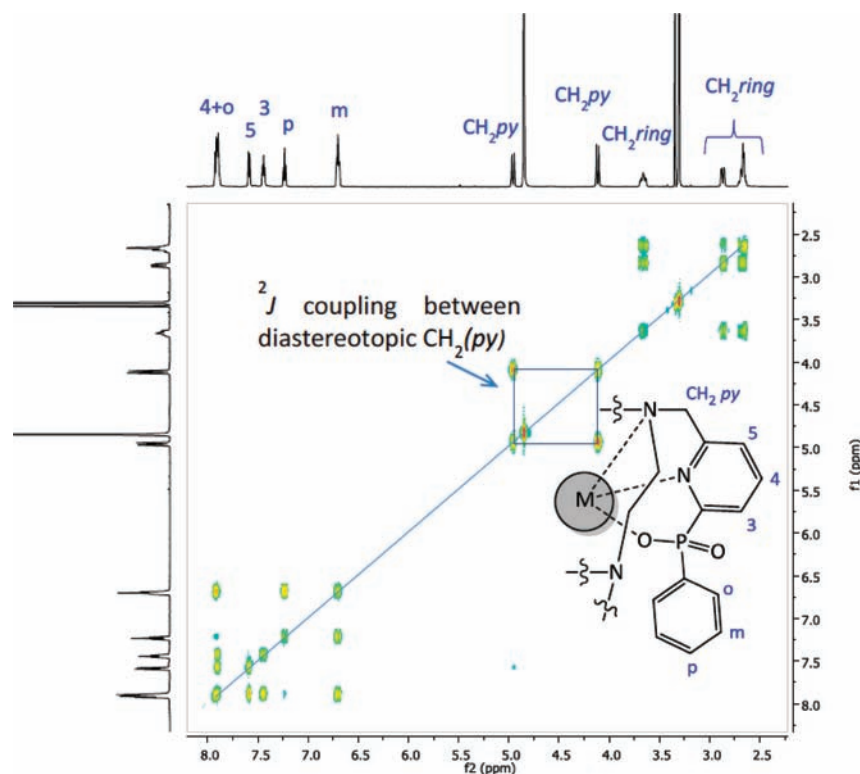


Figure 2. ^1H NMR COSY spectrum for $[\text{YL}^1]$ (295 K, CD_3OD , 500 MHz).

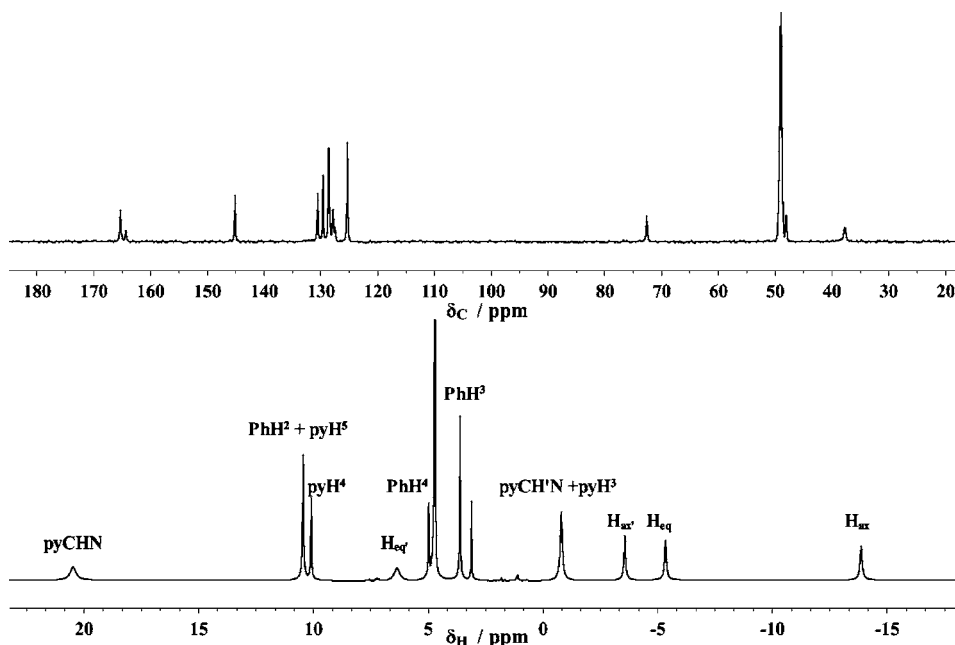


Figure 3. ^1H and ^{13}C NMR spectra of $[\text{YbL}^1]$ (11.7 T, CD_3OD , 295 K): the pro-(*S*)-pyridyl CHN proton resonates above +20 ppm. The phenyl ring (Ph) resonances are labeled 2, 3, and 4 for ortho, meta, and para.

change with increasing temperature (Supporting Information: 276–323 K), notwithstanding the temperature dependence of the dipolar shift. A linear variation of δ_{H} with T^{-2} was observed for each methylene proton, agreeing with a dominant pseudocontact contribution to the paramagnetic shift.¹⁵

Taken together, the observed temperature dependence of the NMR spectra for the yttrium, europium, and ytterbium complexes is consistent with the presence of a single isomeric species in solution, in which ring inversion and arm rotation are

slow on the NMR time scale. The absence of ring inversion distinguishes these conformationally rigid triazacyclononane systems from analogues based on cyclen, where ring inversion typically occurs at a rate of 100 Hz at 298 K.¹⁶

^1H NMR Relaxation Analysis. The gadolinium complexes of L^1 , L^2 , and L^3 in water function as purely “outer-sphere” MR contrast agents because they lack a coordinated water molecule. The low water solubility of $[\text{GdL}^1]$ meant that 10% methanol was added to allow comparative analyses; relaxivities (298 K, 20

MHz) were 0.58, 1.93, and 2.20 $\text{mM}^{-1} \text{s}^{-1}$ respectively, reflecting the relative hydrophobicity of the complexes. The particularly low value for $[\text{GdL}^1]$ suggests preferential local solvation of the complex by the added methanol. The field and temperature dependence of the paramagnetic relaxivity, r_{1p} , of $[\text{GdL}^2]$ was examined in more detail (Figure 4 and Table 3).

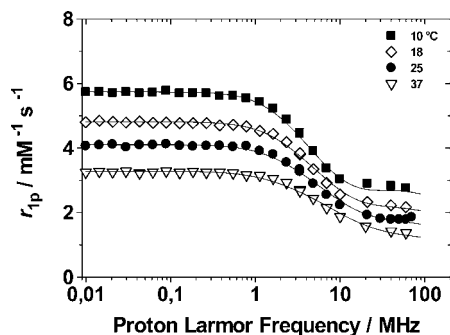


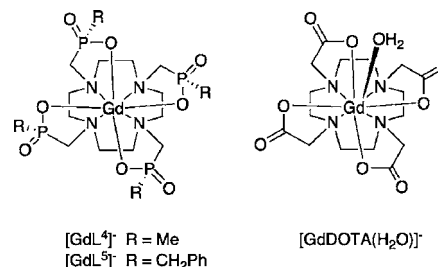
Figure 4. ^1H NMRD profiles for $[\text{GdL}^2]$ (283–310 K), showing the fit (line) to the data points.

Comparisons were made with the gadolinium complexes of the related $q = 0$ tetraphosphinate complexes $[\text{GdL}^4]^-$ ($R = \text{Me}$) and $[\text{GdL}^5]^-$ ($R = \text{PhCH}_2$),^{4a,13} and with $[\text{GdDOTA}(\text{H}_2\text{O})]^-$, for which the putative “outer-sphere” contribution to the measured relaxivity has been assessed (Chart 2).

The outer-sphere mechanism of relaxation involves electron–nuclear magnetic dipole coupling, occurring when the solvent molecules approach the metal center during their translational diffusive motion. It is generally described by Freed’s analysis¹⁷ and depends upon the translational diffusion coefficient, D , the distance of closest approach, a , and the electronic relaxation times, $T_{1,2e}$. It is customary to describe the electron-spin relaxation (ESR) of gadolinium(III) as primarily arising from modulation of the transient zero-field splitting (ZFS) due to distortional motion. In this model, $T_{1,2e}$ is given in terms of the mean-squared fluctuation of ZFS, Δ^2 , and of the correlation time, τ_v , associated with these distortional motions, e.g., a fluctuation in the metal complex coordination polyhedron resulting from solvent collisions.^{17d}

The low-field relaxivity of $[\text{GdL}^2]^-$ (0.01 to ~ 6 MHz) is relatively high because of the small values of Δ^2 and τ_v , consistent with a long electronic relaxation time at zero field, $\tau_{s0} \{1/\tau_{s0} = [\Delta^2[4S(S+1) - 3]\tau_v]/5\}$.^{17c} Only $[\text{GdDOTA}]^-$ and related complexes show lower or comparable values for these parameters. The high field relaxivity (>10 MHz) is relatively low because of the longer value of the distance a between outer-sphere water molecules and the Gd^{III} ion. The

Chart 2. Structures of Gadolinium Complexes



temperature dependence of the relaxivity allowed an estimation of the enthalpy change associated with solvent diffusion, and a value for ΔH_D of $-24.8 (\pm 0.5) \text{ kJ mol}^{-1}$ was found, based on a standard Eyring analysis (see the Supporting Information).

The X-band ESR spectrum of $[\text{GdL}^2]$ was recorded at four temperatures (284–307 K, center field 0.33 T). The X-band (0.34 T) line width (G) values vary markedly among different complexes, reflecting the difference in their electronic relaxation times. At room temperature, the line width of $[\text{GdL}^2]$ is 117 G, similar to that of $[\text{GdDOTA}]^-$ (91 G) and significantly lower than that for $[\text{GdDTPA}]^{2-}$ (604 G).^{18a} From the bandwidth, the electronic relaxation time T_{2e} was calculated (Supporting Information), using simplifications introduced by Reuben^{18b} and adapted by Merbach et al.^{18c} A T_{2e} value of 560 ps was estimated for $[\text{GdL}^2]$ at 296.5 K, compared to values of 745 and 103 ps for $[\text{GdDOTA}]^-$ and $[\text{GdDTPA}]^{2-}$, respectively, measured under the same conditions. The former measurement compares favorably to the value of 450 ps estimated from fitting the VT NMRD profiles, using the Morgan equation,^{17c} shown in eq 1 in a form suitable for gadolinium.

$$\left(\frac{1}{T_{2e}}\right) = \Delta^2 \tau_v \left[\frac{5.26}{1 + 0.372 \omega_S^2 \tau_v^2} + \frac{7.18}{1 + 1.24 \omega_S \tau_v} \right] \quad (1)$$

On the other hand, $[\text{GdL}^3]$ was found to exhibit exceedingly sharp ESR lines (9G at 9 GHz), indicating remarkably slow transverse electron spin relaxation.^{20f} This was tentatively linked to the presence of a rather symmetrical structure and the occurrence of a remarkably small static ZFS. The latter feature is presumably correlated with the nature of the metal coordination environment and explains the difference in the ESR data between $[\text{GdL}^2]$ and $[\text{GdL}^3]$. In fact, there has been much speculation about the determinants of Ln ion electronic relaxation in solution, with suggestions of links to the local metal-ion symmetry and overall complex rigidity.^{18,19} There must be some mechanism that allows coupling of the electron magnetic moment with the surrounding “lattice”, as was

Table 3. Relaxation Parameters^a for $[\text{GdL}^2]$, $[\text{GdL}^4]^-$, $[\text{GdL}^5]^-$, and $[\text{GdDOTA}]^-$ (298 K, H_2O)

“outer-sphere” parameters	$[\text{GdL}^4]^-$	$[\text{GdL}^5]^-$	$[\text{GdL}^2]$	$[\text{GdDOTA}]^-$
r_{1p}^{20} ($\text{mM}^{-1} \text{s}^{-1}$)	2.44	1.85	1.93	2.33
Δ^2 ($\times 10^{19} \text{s}^{-2}$)	7.1 (± 0.1)	7.1 (± 0.1)	2.7 (± 0.1)	1.2
τ_v (ps)	10 \pm 1	12 \pm 1	10 (\pm 1)	11
q^b	0	0	0	
a (Å)	3.6 (± 0.1)	4.3 ^b	4.3 (± 0.1)	4.0 ^b
D ($\times 10^5 \text{cm}^2 \text{s}^{-1}$) ^b	2.24	2.24	2.24	2.24

^aIn comparison, Mazzanti et al.^{3b} report data (298 K) for $[\text{GdL}^3]$ as follows, based on NMRD fitting analysis: $\Delta^2 = 10 \times 10^{19} \text{s}^{-2}$ (fixed); $\tau_v = 0.4$ ps; $a = 4.2$ Å; $T_{1e} = 2500$ ps; $T_{2e} = 2000$ ps. The low-field relaxivity for $[\text{GdL}^2]$ at 298 K is $5.3 \text{ mM}^{-1} \text{s}^{-1}$ (vs $4.0 \text{ mM}^{-1} \text{s}^{-1}$ for $[\text{GdL}^2]$). Low-field relaxivities for $[\text{GdL}^4]^-$ and $[\text{GdL}^5]^-$ at 298 K are 4.2 and $3.1 \text{ mM}^{-1} \text{s}^{-1}$.^{4a,13} ^bFixed in the fitting.

originally suggested by Orbach and co-workers.^{19b} The sensitivity to the coordination environment for gadolinium complexes is evident from the results described here, given the reduction in T_{1e}/T_{2e} caused by permuting a carboxylate for a phosphinate group in $[\text{GdL}^2]$ versus $[\text{GdL}^3]$ and comparing data for $[\text{GdL}^4]^-$ and $[\text{GdL}^5]^-$ versus $[\text{GdDOTA}(\text{OH}_2)]^-$ (vide infra). Aside from the obvious steric change, a major difference between a conjugated carboxylate O and a tetrahedral phosphinate O donor is their difference in polarizability.²⁰ This changes the strength of Ln^{3+} -to-ligand interaction, for example. Differences in T_{1e}/T_{2e} values for carboxylate and phosphonate analogues (n.b. not phosphinate) have been noted earlier in structurally related gadolinium complexes.^{20b,c} It had been suggested that phosphonate groups in mono- and tetrasubstituted complexes give rise to large ZFS amplitudes.^{20d,e} This hypothesis was put forward to explain their small relaxivity values at low magnetic field, associated with relatively fast electron spin relaxation.

Thus, we conclude that the nature of the ligand donor atoms must perturb the f-electron–nuclear interaction and thereby influence the value of T_{1e}/T_{2e} . The effect of permuting donor atom polarizability in a common symmetry can also be examined by analysis of the europium emission spectral form and is discussed below.

³¹P NMR Relaxation Analysis. Compared to Gd, the other paramagnetic Ln ions possess electronic relaxation times that are about 1000 times smaller. This allows NMR spectra to be obtained more easily, without the severe line broadening that inhibits such studies with gadolinium complexes. For these complexes, the primary contribution to longitudinal and transverse relaxation arises from the rotational and conformational modulation of the electron–nuclear dipolar interaction (eqs 2 and 3).²¹

$$R_1 = \frac{1}{15} \left(\frac{\mu_0}{4\pi} \right)^2 \frac{\gamma_N^2 \mu_{\text{eff}}^2}{r^6} \left[\frac{7\tau_{R+e}}{1 + \omega_e^2 \tau_{R+e}^2} + \frac{3\tau_{R+e}}{1 + \omega_N^2 \tau_{R+e}^2} \right] + \frac{2}{5} \left(\frac{\mu_0}{4\pi} \right) \frac{\omega_N^2 \mu_{\text{eff}}^4}{(3kT)^2 r^6} + \frac{3\tau_R}{1 + \omega_N^2 \tau_R^2} \quad (2)$$

$$R_2 = \frac{1}{15} \left(\frac{\mu_0}{4\pi} \right)^2 \frac{\gamma_N^2 \mu_{\text{eff}}^2}{r^6} \left[4\tau_{R+e} + \frac{3\tau_{R+e}}{1 + \omega_N^2 \tau_{R+e}^2} + \frac{13\tau_{R+e}}{1 + \omega_e^2 \tau_{R+e}^2} \right] + \frac{1}{5} \left(\frac{\mu_0}{4\pi} \right)^2 \frac{\omega_N^2 \mu_{\text{eff}}^4}{(3kT)^2 r^6} + \left[4\tau_R + \frac{3\tau_R}{1 + \omega_N^2 \tau_R^2} \right] \quad (3)$$

where μ_0 is vacuum permeability, γ_N is the magnetogyric ratio of the nucleus (in this case ³¹P), r is the electron–nuclear distance, τ_R is the rotational correlation time, ω_N is the nuclear Larmor frequency, T is the absolute temperature, k is the Boltzmann constant, and the remaining symbols are defined as follows:

$$\mu_{\text{eff}}^2 = g_e^2 \mu_B^2 \langle \hat{S}^2 \rangle \quad \tau_{R+e} = (\tau_R^{-1} + T_{1e}^{-1})^{-1}$$

in which g_j is the effective electron g factor, μ_B is the Bohr magneton, $J(J+1)$ is the effective electron angular momentum averaged over the thermally populated electronic energy levels, and T_{1e} is the longitudinal relaxation time of the electron spin. In eqs 2 and 3, the first term arises from modulation of the electron–nuclear dipolar interaction by molecular rotation and random jumps of the electron magnetization; the second term arises from rotational modulation of the dipolar interaction of the nucleus with the average magnetic dipole moment induced in the electron shell by the applied magnetic field. This is often termed Curie relaxation.²²

With the series of $[\text{LnL}^1]$ complexes, ³¹P NMR relaxation rate measurements have been undertaken at five different magnetic fields. Because R_1 is field-dependent through the Curie term, this allows global minimization methods to be undertaken, analyzing sets of data for several lanthanide complexes in parallel. This allows estimates to be made of τ_R , T_{1e} , μ_{eff} and the internuclear separation r . A similar approach has been used recently in ¹⁹F NMR analyses of paramagnetic lanthanide complexes.²¹ The R_1 values for $[\text{LnL}^1]$ (Ln = Eu, Tb, Dy, Ho, Er, Tm, Yb) were measured at 295 K (taking care to measure the temperature accurately in each case, calibrating against an ethylene glycol ¹H shift thermometer) at fields ranging from 4.7 to 16.5 T (Table 4).

Table 4. ³¹P NMR Chemical Shift and Longitudinal Relaxation Rate Data for $[\text{LnL}^1]$ (CD_3OD , 295 K, 1 mM Complex)

Ln ion	δ_p/ppm^a	R_1/Hz				
		4.7 T	9.4 T	11.7 T	14.1 T	16.5 T
Eu	+16.6	3	8	11	14	19
Tb	−35.7	242	603	824	1071	1322
Dy	−15.9	332	876	1213	1619	1978
Ho	−24.6	247	701	1026	1341	1709
Er	−10.5	249	533	745	963	1202
Tm	+8.4	64	194	271	358	463
Yb	+17.7	11	24	34	42	54

^aChemical shift values for Y, Ce, Pr, and Nd were +23.3, +27.8, +31.3, and +21.0 ppm, respectively; the Y complex has an R_1 value of 0.35 Hz (4.7 T).

Minimization of the collective data (excluding Eu) allowed values of τ_R , T_{1e} , μ_{eff} and the internuclear Ln–P separation, r , to be estimated; it was assumed that the values of τ_R and r were the same for each complex. The values obtained (Table 5 and Figure 5) were associated with a global minimum, where $\tau_R = 328 (\pm 13)$ ps and $r = 3.71 (\pm 0.20)$ Å.

The distance r is longer than that revealed in the solid state by X-ray analysis (Table 1) by 0.2 Å on average but falls within 2 standard deviations of the estimated distance. In part, this may reflect the different temperatures of the solution and solid-state analyses (295 vs 120 K). Calculated magnetic moments (Table 5) were systematically lower than those reported in the literature²⁴ but also lie within the errors of this analysis. Attempts were made to fix r as 3.50 Å, but this led to significantly lower (>10%) estimated values of T_{1e} and μ_{eff} with a much less good fit to the data. Similarly, when holding values of μ_{eff} constant, using the data shown in Table 5, no satisfactory convergence was reached.

The values of T_{1e} obtained are compared (Table 5) to those reported²³ for the C_3 -symmetric complex of $[\text{Ln}(\text{dpa})_3]^{3-}$, the only system that has been studied that shares a common

Table 5. Estimated Electronic Relaxation Times T_{1e} and Magnetic Moments μ_{eff} for $[\text{LnL}^1]$, Derived from Global Minimization^c of the Relaxation Rate Field Dependence [295 K, CD_3OD ; $r = 3.71 (\pm 0.20)$ Å, $\tau_{\text{R}} = 328 (\pm 13)$ ps]

Ln	$T_{1e}/\text{ps} (\pm 0.03)^a$	$\mu_{\text{eff}}/\mu_{\text{B}} (\pm 0.62)^b$
Tb	0.28 (0.29)	9.2 (9.8)
Dy	0.26 (0.45)	10.2 (10.3)
Ho	0.13 (0.17)	9.8 (10.4)
Er	0.31 (0.32)	8.9 (9.4)
Tm	0.06 (0.16)	7.1 (7.6)
Yb	0.07 (0.10)	4.1 (4.3)

^aValues in parentheses refer to the C_3 -symmetric trischelate complex of dpa.²³ ^bTypical literature values for the Ln^{III} ions are reported in parentheses.²⁴ ^cThe error for the minimization function was 1×10^{-4} , which was the lowest value for any fitting attempted.

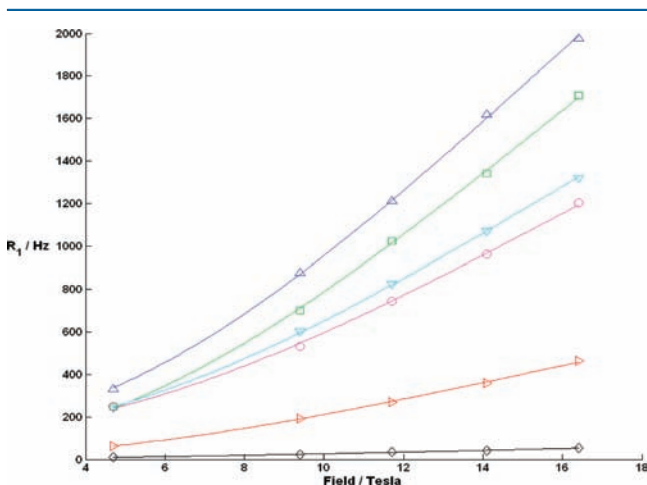


Figure 5. Variation of R_1 with field for the lanthanide complexes shown, showing the best fit (line) to the experimental data (295 K, CD_3OD): in sequence, from the top, for the faster relaxing system, Dy, Ho, Tb, Er, Tm, and Yb. Errors in the R_1 values lie within the data point symbols.

symmetry and an isostructural nine-coordinate coordination environment, notwithstanding their differing donor sets, i.e., N_3O_6 for $[\text{Ln}(\text{dpa})_3]^{3-}$ instead of N_6O_3 for $[\text{LnL}^1]$. Reasonable agreement is found, although the values of T_{1e} for the phosphinate system are systematically lower than those for the hexacarboxylate series.

A similar trend was apparent in comparing values of T_{1e}/T_{2e} for the gadolinium complexes of the various carboxylate and phosphinate complex analogues detailed above. Certainly, the electronic relaxation times for the non-gadolinium lanthanide complexes reported here are too short to suggest a simple coupling of the electron magnetic moment to ligand vibrations and rotations. Modulation of the ZFS has been suggested to determine the electronic relaxation for lanthanide systems, induced by solvent collisions.^{19b} Overall, the data reported here for Tb–Yb do not unravel the determinants of electronic relaxation but strongly suggest that the nature of the metal coordination environment is important, i.e., the nature and polarizability of the ligand donor set, as suggested for the much more slowly relaxing gadolinium examples. Furthermore, the local steric demand imposed by the ligand is very likely to influence the extent of local librational motion, contributing to the transient ZFS.

Lanthanide Optical Emission Measurements. Absorption and emission spectral data for selected lanthanide complexes have been examined in water and D_2O (Table 6).

Table 6. Absorption and Emission Spectral Data for Selected $[\text{LnL}^1]$ and $[\text{LnL}^2]$ Complexes (H_2O , 295 K, pH 5.8)

complex	$\lambda_{\text{abs}}/\text{nm}$	$\epsilon/\text{M}^{-1}\text{cm}^{-1}$	$\tau(\text{H}_2\text{O})/\text{ms}$	$\tau(\text{D}_2\text{O})/\text{ms}$	$\phi_{\text{em}}^{\text{Ln}}/\%$ ($\pm 15\%$)
$[\text{SmL}^1]$	274	14600	0.03	0.04	0.7
$[\text{EuL}^1]$	274	14000	1.36	1.54	9
$[\text{EuL}^2]$	272	8400	1.56	1.60	7
$[\text{TbL}^1]$	274	13800	2.16	2.51	50
$[\text{TbL}^2]$	272	7500	2.59	2.98	60
$[\text{DyL}^1]$	274	14400	0.04	0.04	2.9

The $\pi-\pi^*$ transitions in the pyridyl chromophore are associated with the lowest electronic energy band at 274 nm. Each Ln ion is effectively shielded from the solvent, and the modest increases in the metal excited-state lifetime are consistent with a solution hydration state, $q = 0$, in each case.²⁵ The overall metal-based emission quantum yields follow the order $\text{Tb} > \text{Eu} > \text{Dy} > \text{Sm}$, reflecting the well-established relative efficiencies of intramolecular energy transfer, the degree of quenching of the intermediate pyridyl singlet excited state by electron transfer to the metal ion ($\text{Eu} > \text{Sm} > \text{Dy/Tb}$), and the sensitivity of the emissive excited state to vibrational deactivation by energy-matched oscillators, e.g., CH , $\text{C}=\text{O}$. The higher values for the terbium complexes are in line with those reported for $[\text{TbL}^3]$,^{3b,c} consistent with a particularly efficient energy transfer to higher-lying terbium excited states from the pyridyl triplet. The quantum yield value for $[\text{DyL}^1]$ is among the highest reported for any dysprosium complex in water;¹ for example, it is more than twice that reported for a tetra(hydroxyisophthalamide) system.²⁶

Emission spectra for $[\text{LnL}^1]$ ($\text{Ln} = \text{Dy}, \text{Tb}, \text{Sm}, \text{Eu}$) show the expected emission profiles (Figure 6), and spectra for the europium complexes of L^1 and L^2 were identical in form. The europium spectrum was also measured at 10 K in a frozen glass, using excitation at 365 nm (see the Supporting Information). The solution and “solid-state” emission spectra were nearly identical and did not change markedly in form or the relative intensity with temperature.

The spectral form of $[\text{EuL}^{1-3}]$ very strongly resembles that of $[\text{Eu}(\text{dpa})_3]^{3-}$ ²⁷ with a ratio of intensities of the $\Delta J = 2/\Delta J = 1$ bands on the order of 4:1 in each case. This contrasts with the behavior of the C_3 -symmetric complex $[\text{Eu}(\text{ODA})_3]^{3-}$ (ODA = oxidiacetate),²⁸ in which the same number of transitions is observed in each manifold but with a $\Delta J = 2/\Delta J = 1$ intensity ratio of nearly unity. In europium emission spectra, the oscillator strength of the $\Delta J = 1$ transition is magnetic-dipole-allowed and independent of the ligand environment. In contrast, the $\Delta J = 2$ transition is electric-dipole (ED)-allowed and hypersensitive to ligand perturbation. This behavior is conventionally explained using the ligand polarization model,²⁹ wherein electric-quadrupole-allowed transitions (such as 5D_0 to 7F_2) gain significant ED strength via a quadrupole (Ln^{3+})-induced dipole (ligand) mechanism of coupling. Induced dipoles on the ligands are created by direct coupling to the ED components of the radiation field. Thus, 4f–4f ED strength has been related to ligand dipolar polarizabilities and to the anisotropies of these polarizabilities.³⁰ Evidently, among the ligand donors examined here, the polarizable pyridyl groups in

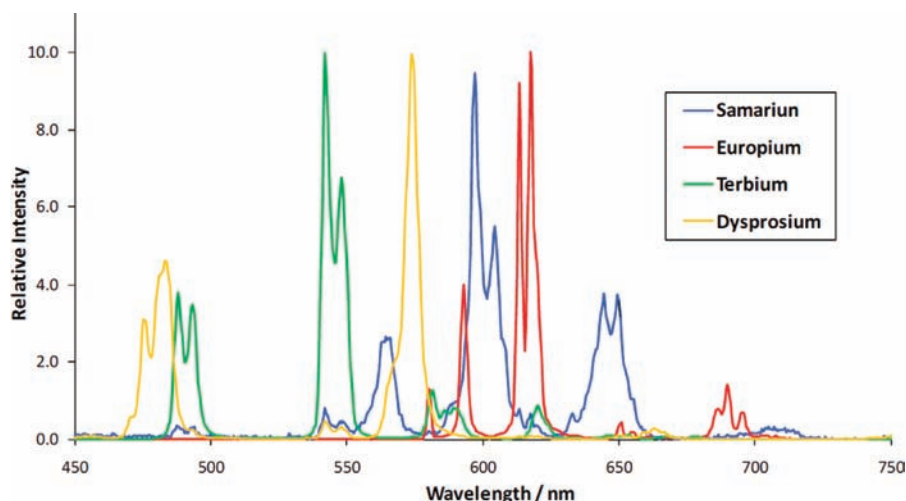


Figure 6. Emission spectra for $[\text{LnL}^1]$ in water (295 K); spectra have been scaled in intensity.

L^{1-3} and in dpa are common and, to a first-order approximation, define the intensity of the $\Delta J = 2$ transition. Comparing $[\text{EuL}^1]$ and $[\text{EuL}^3]$, measured under the same solution conditions, very similar spectra were observed (see the Supporting Information), but the $\Delta J = 2/\Delta J = 1$ intensity ratio was about 20% higher for $[\text{EuL}^3]$. This increase can be attributed to the greater polarizability of the carboxylate versus phosphinate O atoms, consistent with the importance of this property in determining the electronic relaxation rates in their gadolinium complexes, *vide supra*.

As discussed in the preliminary communication, $[\text{EuL}^1]$ could be resolved on a chiral HPLC column, and the configuration of the separated enantiomers was assigned by CD methods.⁶ The same method was attempted with $[\text{EuL}^2]$ and $[\text{EuL}^3]$. In every case, baseline separation was achieved, although the enantiomeric SSS- Δ and RRR- Λ complexes of $[\text{EuL}^2]$ were resolved with a reduced separation ($\Delta t_r = 0.5$ vs 1.8 min for $[\text{EuL}^1]$, CHIRALPAK-IC, 288 K, EtOH/MeOH/Et₂NH, 50:50:1). Each resolved complex showed circularly polarized luminescence (CPL) spectra that did not change after heating in methanol at 50 °C for 48 h, indicating a resistance to racemization. The ability to separate the enantiomeric Δ/Λ isomers is consistent with ¹H NMR evidence for a very large barrier to Δ/Λ interconversion at 323 K.

The CPL spectra for $[\text{EuL}^1]$ and $[\text{EuL}^2]$ were identical in form, giving mirror-image spectra for the resolved complexes (Figure 7 and the Supporting Information). These spectra particularly highlight the five allowed transitions in the complex $\Delta J = 4$ manifold (*viz.* Figure 6) and clarify the nature of the

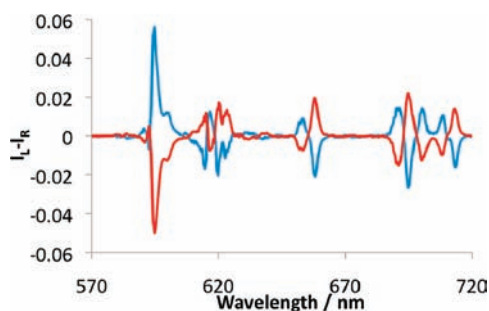


Figure 7. CPL spectra for (RRR)- Λ - $[\text{EuL}^1]$ (red) and (SSS)- Δ - $[\text{EuL}^1]$ (blue; H₂O, 295 K).

transitions in the $\Delta J = 1$ manifold. In the latter case, these transitions are not well resolved in the total emission spectrum, but in the CPL, a weak A_1-A_2 transition is observed at 591 nm, and the two Zeeman components (at 595 and 600 nm) of the A_1-E transition are clearly resolved, with the higher-energy component being more intense.

Molecular Quadratic Hyperpolarizability. The second-order nonlinear optical properties of the isostructural series of $[\text{LnL}^1]$ complexes were examined in a methanol solution, using the hyper-Raleigh light-scattering (HLS) technique. The HLS technique involves the detection of an incoherently scattered harmonic, generated by irradiation of a solution of the complex with a laser of wavelength λ . This leads to the measurement of the mean value of the $\beta \times \beta$ tensor product, $\langle \beta_{\text{HLS}} \rangle$.^{31,7-10} The quadratic hyperpolarizability is the sum of the dipolar and octupolar contributions, and the HLS method measures this total.

Measurements were carried out as reported by Zyss, using 1 mM solutions of the complex. The magnitude of $\beta^{1,064}$ (in 10⁻³⁰ esu) increased from 149 for Ce to 494 for Dy, before falling again toward Lu; the value for Y (4f⁰) was only slightly lower than the value for Yb (4f¹⁴). These $\langle \beta_{\text{HLS}} \rangle$ values are 2 orders of magnitude larger than the values reported for $[\text{Ln}(\text{dpa})_3]^{3-}$ in water (298 K, 0.1 M solution),^{7a} where a steady increase was reported across the series. This variation was attributed to polarization of the f electrons by the local ligand in such complexes.

On the other hand, Zyss et al. has more recently reported⁸ that, for lanthanide complexes of tris-(hexafluoroacetylacetonate)diglyme in a chloroform solution, the dominant contribution to $\langle \beta_{\text{HLS}} \rangle$ arose from the octupolar term, and it was only the much smaller (1% of total) dipolar term that increased as a function of the number of f electrons, across the series. It has also been noted that, in oligomeric lanthanide tris(cinnamic acid) complexes in the solid state,⁹ the $\langle \beta_{\text{HLS}} \rangle$ values reach a maximum near the center of the series before falling (Figure 8). The data reported here reveal very large values for $\langle \beta_{\text{HLS}} \rangle$, apparently larger than those for any other lanthanide complex reported in solution and 2 orders of magnitude greater than those for the series of $[\text{Ln}(\text{dpa})_3]$ complexes.⁷ This behavior clearly suggests a dominant octupolar contribution to the measured hyperpolarizability. Why these systems differ so markedly in their behavior

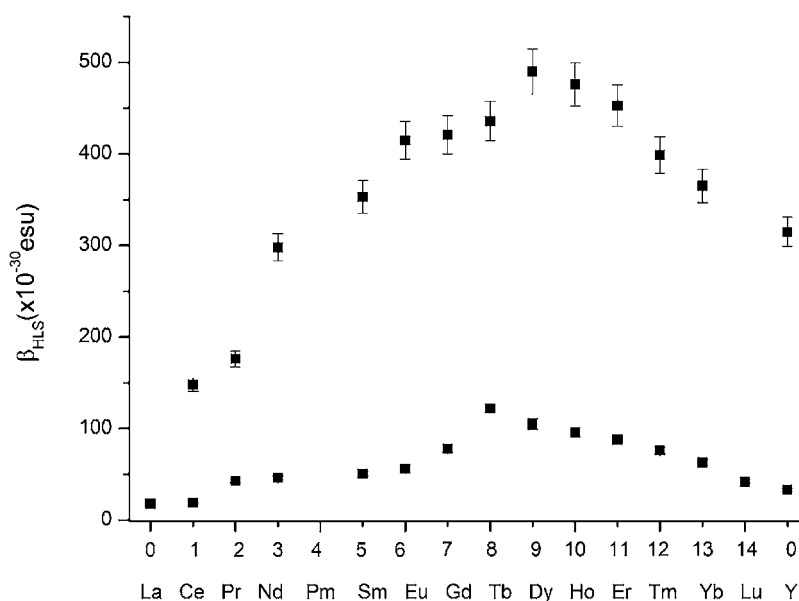


Figure 8. Molecular polarizabilities $\langle\beta_{\text{HLS}}\rangle$ of $[\text{LnL}^1]$ complexes (upper) in a methanol solution (1 mM complex, 298 K, $\lambda = 1064$ nm). Values for the tris(cinnamate) complexes reported by Tanner et al.⁹ are also shown (lower).

compared to the $[\text{Ln}(\text{dpa})_3]^{3-}$ series of complexes remains unclear.

CONCLUSIONS

The lanthanide complexes of L^1 and L^2 form an isostructural series in the solid state. The solvent is excluded from the primary coordination environment, and the additional steric bulk created by the presence of three phosphinate substituents with a common configuration at phosphorus shields the face opposite the triazacyclononane ring, further screening the Ln ion. This leads to further exclusion of the solvent molecules from the vicinity of the Ln ion, minimizing the second sphere of hydration. This is revealed in the very low relaxivity of the gadolinium complexes in aqueous media and also leads to the suppression of deactivation of the emissive lanthanide excited state by vibrational energy transfer to solvent oscillators. Thus, the overall emission quantum yields are very high for the terbium, samarium, and dysprosium complexes in aqueous media, and the excited-state lifetimes are long and do not change significantly in D_2O . The emissive complexes of L^1 and L^2 can be readily modified structurally in the 4 position of the pyridyl ring to allow the introduction of chromophores with extended conjugation that allow efficient sensitized excitation of the Ln ion. This work has been undertaken and will be reported elsewhere shortly.

The emission spectral form of the europium complexes of L^1 , L^2 , and L^3 is very similar. A 20% increase in the relative intensity of the hypersensitive, ED-allowed $\Delta J = 2$ transition is observed for $[\text{EuL}^3]$ compared to $[\text{EuL}^1]$ and $[\text{EuL}^2]$. This change in the spectral form is ascribed to an increase in the polarizability of carboxylate versus phosphinate O donors. Each series of complexes can be resolved by chiral HPLC, and the resolved SSS- Δ and RRR- Λ enantiomers do not undergo racemization after 48 h at 50 °C in solution, paving the way for future chiroptical studies of the separated Δ and Λ enantiomers and their homologues.

The molecular quadratic hyperpolarizability of $[\text{LnL}^1]$ in a methanol solution revealed high values for $\langle\beta_{\text{HLS}}\rangle$, reaching a maximum value of around 500×10^{-30} esu at the center of the

lanthanide series. Such high values are unprecedented for lanthanide complexes in solution and may be compared to values that are 2 orders of magnitude lower for the C_3 -symmetric isostructural series of $[\text{Ln}(\text{dpa})_3]$ complexes. The quadratic hyperpolarizability is deduced to be dominated by the octupolar term, rather than the dipolar term, and shows no simple relationship to the number of f electrons. These findings lend support to the hypothesis promulgated recently by Zyss et al.⁸ that rationalizes reports of a linear variation of $\langle\beta_{\text{HLS}}\rangle$ with the number of f electrons as being manifested only through the dipolar contribution to the total hyperpolarizability.

VF and VT NMR measurements allowed an assignment of the ^1H NMR spectra of the europium and ytterbium complexes. This analysis established the common C_3 -symmetric structure of this series of complexes in solution. VT studies showed that the rates of inversion of the triazacyclononane ring and rotation of the pendant arms about the C_3 axis were slow on the NMR time scale at ambient temperature, consistent with the rigid solution structure of these complexes. VF measurements of the ^{31}P NMR T_1 values for the series of terbium to ytterbium complexes of L^1 enabled global minimization methods to be used to estimate the rotational correlation time of the complex, τ_R , the effective magnetic moment, μ_{eff} , and the individual lanthanide electronic relaxation times, T_{1e} . The latter values fell in the range 0.06–0.31 ps and showed variation with the nature of the Ln ion that was similar to the early data of Williams et al.²³ for the C_3 -symmetric lanthanide complexes of 2,6-pyridinedicarboxylate, $[\text{Ln}(\text{dpa})_3]$. For $[\text{GdL}^1]$, estimates of electronic relaxation times were made from VT EPR measurements and also by analysis of the temperature dependence of the NMRD profile that defines the water proton relaxivity of aqueous solutions of the complex. Values of T_{1e} (T_{1e} approximates to T_{2e} in this case) were of the order of 500 ps in each case. These values are systematically lower than those found for structurally related complexes with carboxylate donors.²⁰ Variation in the electronic relaxation times for Gd and the much more rapidly relaxing Tb, Dy, Ho, Er, Tm and Yb ions is linked to the change in the ligand donor polarizability. This structure–property relationship may be tentatively

compared to the changes in the relative emission intensity found for the hypersensitive, ED-allowed transitions of the corresponding europium(III) complexes that are known to depend on the ligand donor polarizability.

EXPERIMENTAL SECTION

Synthesis and Purification. Reagent-grade chemicals 2-bromo-6-methylpyridine, Ln(OAc)₃ (Sigma Aldrich), MeP(OEt)₂ (Strem), and 1,4,7-triazacyclononane (ChemaTech) were used as received. Acetonitrile was distilled from calcium hydride. Distilled and Millipore-filtered water was used in all reactions. Reactions were carried out under an atmosphere of dry argon. Thin-layer chromatography (TLC) was carried out on silica plates (Merck 5554) or neutral alumina oxide plates (Merck Art 5550) and visualized under irradiation at 254 nm or iodine staining. Preparative column chromatography was carried out using silica (Merck Silica Gel 60; 230–400 mesh) or neutral aluminum oxide (Merck Aluminum Oxide 90, types II and III, 70–230 mesh), soaked in ethyl acetate prior to use.

Chiral HPLC analyses of [Euⁿ] (*n* = 1, 2 or 3) were attempted using a Chiralpak IC column, eluted using an isocratic gradient with a solvent system composed of EtOH/MeOH/HNEt₂ (50/50/0.1) at 15 °C; the enantiomeric complexes of [EuL¹] eluted with Δ*t_R* = 1.6 min using a flow rate of 1 mL min⁻¹. Analytical reverse-phase HPLC analysis was performed at 298 K on a Perkin-Elmer system, with an XBridge C-18 10 cm/3.5 μm column at a flow rate of 1 mL min⁻¹, using the method given in Table 7.

Table 7

time/min	H ₂ O + 0.1% HCO ₂ H	CH ₃ CN + 0.1% HCO ₂ H
0	95	5
1	95	5
9	0	100
11	0	100
12	95	5
13	95	5

Ethyl (6-Methylpyridin-2-yl)(phenyl)phosphinate (1). 2-Bromo-6-methylpyridine (3.00 g, 17.4 mmol), ethyl phenylphosphinate (3.56 g, 20.9 mmol), and triethylamine (10 mL, 71 mmol) were added to dry degassed (freeze–thaw cycle) toluene (30 mL). Tetrakis(triphenylphosphine)palladium(0) (320 mg, 0.27 mmol) was added, and the mixture was degassed three times before being stirred at 125 °C for 16 h under argon. The solution was diluted with CH₂Cl₂ (50 mL), washed with HCl (1 M, 2 × 60 mL) and water (3 × 60 mL), dried over K₂CO₃, and filtered and the solvent removed under reduced pressure to give a dark residue. Purification by column chromatography on silica (CH₂Cl₂/0.5% MeOH) gave a colorless oil (3.1 g, 66%). ¹H NMR (CDCl₃, δ): 8.01 (2H, dd, ³J = 8.0 Hz, ³J_{H–P} = 12.0 Hz, H^o), 7.91 (1H, dd, ³J = 7.0 Hz, ³J_{H–P} = 14.0 Hz, H³), 7.67 (1H, td, ³J_{H–H} = 7.0 Hz, ⁴J_{H–P} = 3.0 Hz, H⁴), 7.54 (1H, t, ³J = 8.0 Hz, H^p), 7.48 (2H, td, ³J = 8.0 Hz, ⁴J_{H–P} = 4.0 Hz, H^m), 7.23 (1H, d, ³J = 7.0 Hz, H⁵), 4.15 (2H, qd, ³J = 7.0 Hz, ³J_{H–P} = 4.5 Hz, CH₂O), 2.60 (3H, s, H¹), 1.38 (3H, t, ³J = 7.0 Hz, CH₃). ¹³C NMR (CDCl₃, δ): 159.8 (d, ³J_{C–P} = 20 Hz, C⁶), 154.0 (d, ¹J_{C–P} = 167 Hz, C²), 135.8 (d, ³J_{C–P} = 10 Hz, C⁴), 132.6 (d, ²J_{C–P} = 12 Hz, C^o), 132.5 (d, ⁴J_{C–P} = 4 Hz, C^p), 130.6 (d, ¹J_{C–P} = 136 Hz, Cⁱ), 128.5 (d, ³J_{C–P} = 9 Hz, C^m), 125.8 (d, ⁴J_{C–P} = 4 Hz, C^s), 125.6 (d, ²J_{C–P} = 22 Hz, C³), 61.9 (d, ²J_{C–P} = 6 Hz, CH₂O), 24.9 (Me), 16.7 (CH₂Me). ³¹P NMR (CDCl₃, δ): 26.8. HRMS⁺: *m/z* 262.0999 [M + H]⁺ (C₁₄H₁₇O₂NP requires *m/z* 262.0997). *R_f* = 0.37 (silica, CH₂Cl₂/5% MeOH).

Ethyl [6-(Bromomethyl)pyridin-2-yl](phenyl)phosphinate (2). To a solution of ethyl (6-methylpyridin-2-yl)(phenyl)phosphinate (400 mg, 1.53 mmol) in carbon tetrachloride (25 mL) was added *N*-bromosuccinimide (327 mg, 1.84 mmol) and dibenzoyl peroxide (20 mg, 0.8 mmol). The mixture was stirred and irradiated by a 100 W lamp under an argon atmosphere. The reaction was monitored by ¹H

NMR and stopped after 16 h. The solvent was removed under reduced pressure, and the crude product was dissolved in CH₂Cl₂ (20 mL) and washed with a dilute K₂CO₃ solution (20 mL) to remove excess succinimide. The organic layer was dried over MgSO₄ and filtered and the solvent removed under reduced pressure. Purification by column chromatography on silica (CH₂Cl₂/0–1% MeOH using 0.05% increments) yielded a colorless oil (198 mg, 38%). ¹H NMR (CDCl₃, δ): 8.01 (1H, dd, ³J = 7.0 Hz, ³J_{H–P} = 14.0 Hz, pyH³), 8.00 (2H, dd, ³J = 8.0 Hz, ³J_{H–P} = 12.0 Hz, H^o), 7.79 (1H, td, ³J = 7.0 Hz, ⁴J_{H–P} = 3.0 Hz, pyH⁴), 7.53 (1H, t, ³J = 8.0 Hz, H^p), 7.52 (1H, d, ³J = 7.0 Hz, pyH⁵), 7.46 (2H, td, ³J_{H–H} = 8.0 Hz, ⁴J_{H–P} = 4.0 Hz, H^m), 4.57 (2H, s, CH₂Br), 4.13 (2H, qd, ³J_{H–H} = 7.0 Hz, ³J_{H–P} = 4.5 Hz, CH₂O), 1.37 (3H, t, ³J_{H–H} = 7.0 Hz, Me). ¹³C NMR (CDCl₃, δ): 158.0 (d, ³J_{C–P} = 20 Hz, C⁶), 154.7 (d, ¹J_{C–P} = 167 Hz, C²), 137.3 (d, ³J_{C–P} = 10 Hz, C⁴), 132.7 (d, ²J_{C–P} = 12 Hz, C^o), 132.6 (d, ⁴J_{C–P} = 4 Hz, C^p), 130.2 (d, ¹J_{C–P} = 136 Hz, Cⁱ), 128.5 (d, ³J_{C–P} = 9 Hz, C^m), 127.5 (d, ²J_{C–P} = 22 Hz, C³), 125.8 (d, ⁴J_{C–P} = 4 Hz, C^s), 62.1 (d, ²J_{C–P} = 6 Hz, CH₂O), 33.6 (CH₂Br), 16.7 (Me). ³¹P NMR (CDCl₃, δ): 26.0. HRMS⁺: *m/z* 340.0122 [M(⁷⁹Br) + H]⁺ (C₁₄H₁₆O₂NP⁷⁹Br requires *m/z* 340.0102), 342.0098 [M(⁸¹Br) + H]⁺ (C₁₄H₁₆O₂NP⁸¹Br requires *m/z* 342.0088). *R_f* = 0.57 (silica, CH₂Cl₂/5% MeOH).

1,4,7-Tris[ethyl (6-methylpyridin-2-yl)(phenyl)phosphinate]-1,4,7-triazacyclononane (3). 1,4,7-Triazacyclononane (14 mg, 0.11 mmol), ethyl [6-(bromomethyl)pyridin-2-yl](phenyl)phosphinate (130 mg, 0.38 mmol), and K₂CO₃ (51 mg, 0.38 mmol) were stirred in dry CH₃CN (5 mL) at 80 °C for 20 h under argon. The reaction was monitored by TLC to confirm that the brominated starting material had been consumed. The solvent was removed under reduced pressure, and the resultant residue was dissolved in CH₂Cl₂ (30 mL) and washed with water (3 × 30 mL). The organic layer was dried over MgSO₄ and filtered and the solvent removed under reduced pressure. Purification by column chromatography on alumina (CH₂Cl₂/0–2% MeOH in 0.05% increments) gave a glassy, very pale-yellow solid (60 mg, 62%). ¹H NMR (CDCl₃, δ): 7.96 (3H, dd, ³J = 7.0 Hz, ³J_{H–P} = 14.0 Hz, H³), 7.95 (6H, dd, ³J = 8.0 Hz, ³J_{H–P} = 12.0 Hz, H^o), 7.74 (3H, td, ³J = 7.0 Hz, ⁴J_{H–P} = 3.0 Hz, H⁴), 7.54 (3H, d, ³J = 7.0 Hz, H⁵), 7.47 (3H, t, ³J = 8.0 Hz, H^p), 7.39 (6H, td, ³J = 8.0 Hz, ⁴J_{H–P} = 4.0 Hz, H^m), 4.11 (6H, qd, ³J_{H–H} = 7.0 Hz, ³J_{H–P} = 4.5 Hz, CH₂O), 3.83 (6H, br s, CH₂N), 2.74 (12H, br s, ring CH₂N), 1.34 (9H, t, ³J = 7.0 Hz, Me). ¹³C NMR (CDCl₃, δ): 161.7 (d, ³J_{C–P} = 20 Hz, C⁶), 153.9 (d, ¹J_{C–P} = 167 Hz, C²), 136.4 (d, ³J_{C–P} = 10 Hz, C⁴), 132.6 (d, ⁴J_{C–P} = 4 Hz, C^p), 132.5 (d, ²J_{C–P} = 12 Hz, C^o), 130.5 (d, ¹J_{C–P} = 136 Hz, Cⁱ), 128.4 (d, ³J_{C–P} = 9 Hz, C^m), 126.6 (d, ²J_{C–P} = 22 Hz, C³), 125.6 (d, ⁴J_{C–P} = 4 Hz, C^s), 64.1 (CH₂N), 61.8 (d, ²J_{C–P} = 6 Hz, CH₂O), 55.7 (ring NCH₂), 16.7 (Me). ³¹P NMR (CDCl₃, δ): 26.7. HRMS⁺: *m/z* 907.3641 [M + H]⁺ (C₄₈H₅₈O₆N₆P₃ requires *m/z* 907.3631). *R_f* = 0.56 (alumina, CH₂Cl₂/5% MeOH).

[EuL¹]. 1,4,7-Tris[ethyl (6-methylpyridin-2-yl)(phenyl)phosphinate]-1,4,7-triazacyclononane (38 mg, 0.042 mmol) was dissolved in HCl (6M, 8 mL), and the solution was stirred at 100 °C for 16 h. The solvent was lyophilized to give a yellow solid. Hydrolysis of the OEt groups was confirmed by ¹H and ³¹P NMR [δ_p (CDCl₃) 16.0]. The solid was dissolved in H₂O/CH₃OH (1:1, v/v; 6 mL) and the pH of the solution adjusted to 5.8 using NaOH. Eu(OAc)₃ (18 mg, 0.046 mmol) was added, and the solution was stirred at 50 °C for 18 h. After the solution was allowed to cool to room temperature, the pH was raised to 10 by the addition of a dilute aqueous ammonia solution. The solution was stirred for 1 h, causing excess Eu³⁺ to precipitate as Eu(OH)₃, which was removed by syringe filtration. Adjustment of the pH to 5.8 by the addition of CH₃CO₂H, followed by lyophilization of the solvent, gave a solid, which was purified by column chromatography (silica, CH₂Cl₂/20% CH₃OH/1% aqueous NH₄OH) to give a white solid (32 mg, 82%). HRMS⁺: *m/z* 971.1665 [M + H]⁺ (C₄₂H₄₃O₆N₆P₃¹⁵¹Eu requires *m/z* 971.1656). Anal. Calcd for C₄₂H₄₂N₆O₆P₃Eu·3H₂O: C, 49.5; H, 4.71; N, 8.24. Found: C, 49.2; H, 4.97; N, 8.04. ³¹P NMR (CD₃OD, 9.4T, 295 K, δ): +16.6. ¹H NMR (CD₃OD, 9.4 T, 295 K, δ): 7.75 (6H, br s, pyH⁵ + pyH⁴), 7.51 (3H, br s, pyCHN), 7.30 (3H, s, PhH⁴), 7.19 (6H, br s, PhH²), 6.56 (6H, br s, PhH³), 6.20 (3H, br s, pyH³), 4.52 (3H, br s,

NCH'_{eq} , -0.10 (3H, br s, pyCH'N), -0.64 (3H, br s, NCH'_{ax}), -0.93 (3H, br s, NCH_{eq}), -4.79 (3H, br s, NCH_{ax}). UV [H_2O ; λ_{max} nm (ϵ , $\text{M}^{-1} \text{cm}^{-1}$): 274 (14000). $\tau(\text{H}_2\text{O}) = 1.26$ ms, $\tau(\text{D}_2\text{O}) = 1.54$ ms, $\phi_{\text{em}}(\text{H}_2\text{O}) = 9\%$, and $t_{\text{R}} = 6.81$ min.

The following complexes were prepared in an analogous manner and were isolated as colorless solids (unless stated), which gave single peaks on HPLC analysis (λ_{exc} 275 nm) with a retention time of 6.80 (± 0.05) min. ^{31}P NMR relaxation rate data for each lanthanide complex are reported in Table 4.

[CeL¹]: pale-yellow solid (12.2 mg, 77%). Anal. Calcd for $\text{C}_{42}\text{H}_{42}\text{N}_6\text{O}_6\text{P}_3\text{Ce}\cdot 3.5\text{H}_2\text{O}$: C, 49.3; H, 4.79; N, 8.21. Found: C, 49.1; H, 5.05; N, 8.01. ESMS⁺: m/z 960.3 [M (^{140}Ce) + H]⁺. ^{31}P NMR (CD_3OD , 9.4 T, 295 K, δ): +27.8. UV [H_2O ; λ_{max} nm (ϵ , $\text{M}^{-1} \text{cm}^{-1}$): 275 (14500), 340 (120). [PrL¹] (13.3 mg, 84%). ESMS⁺: m/z 961.3 [M (^{141}Pr) + H]⁺. ^{31}P NMR (CD_3OD , 9.4 T, 295 K, δ): +31.3. [NdL¹] (12.7 mg, 80%). ESMS⁺: m/z 964.2 [M (^{144}Nd) + H]⁺. ^{31}P NMR (CD_3OD , 9.4 T, 295 K, δ): +21.0. [SmL¹] (12.5 mg, 78%). ESMS⁺: m/z 972.2 [M (^{152}Sm) + H]⁺. ^{31}P NMR (CD_3OD , 9.4 T, 295 K, δ): +31.4. $\tau(\text{H}_2\text{O}) = 0.03$ ms, $\tau(\text{D}_2\text{O}) = 0.04$ ms, and $\phi_{\text{em}}(\text{H}_2\text{O}) = 0.7\%$. [GdL¹] (13.0 mg, 81%). ESMS⁺: m/z 976.2 [M (^{156}Gd) + H]⁺. $r_{1\text{p}}$ (20 MHz, 298 K, 10% MeOH in H_2O): $0.58 \text{ mM}^{-1} \text{ s}^{-1}$. [TbL¹] (12.6 mg, 78%). ESMS⁺: m/z 979.2 [M (^{159}Tb) + H]⁺. ^{31}P NMR (CD_3OD , 9.4 T, 295 K, δ): -35.7 . $\tau(\text{H}_2\text{O}) = 1.63$ ms, $\tau(\text{D}_2\text{O}) = 1.84$ ms, and $\phi_{\text{em}}(\text{H}_2\text{O}) = 50\%$. [DyL¹] (13.0 mg, 80%). ESMS⁺: m/z 984.2 [M (^{164}Dy) + H]⁺. ^{31}P NMR (CD_3OD , 9.4 T, 295 K, δ): -13.9 . $\tau(\text{H}_2\text{O}) = 0.04$ ms, $\tau(\text{D}_2\text{O}) = 0.045$ ms, and $\phi_{\text{em}}(\text{H}_2\text{O}) = 2.9\%$. [HoL¹] (12.7 mg, 78%). ESMS⁺: m/z 985.3 [M (^{165}Ho) + H]⁺. ^{31}P NMR (CD_3OD , 9.4 T, 295 K, δ): -24.6 . [ErL¹] (14.3 mg, 88%). ESMS⁺: m/z 988.2 [M (^{168}Er) + H]⁺. ^{31}P NMR (CD_3OD , 9.4 T, 295 K, δ): -10.5 . [TmL¹] (12.9 mg, 79%). ESMS⁺: m/z 989.3 [M (^{169}Tm) + H]⁺. ^{31}P NMR (CD_3OD , 9.4 T, 295 K, δ): +8.4.

[YbL¹] (13.6 mg, 83%). Anal. Calcd for $\text{C}_{42}\text{H}_{42}\text{N}_6\text{O}_6\text{P}_3\text{Yb}\cdot 3.5\text{H}_2\text{O}$: C, 47.8; H, 4.64; N, 7.96. Found: C, 47.6; H, 4.47; N, 8.14. ESMS⁺: m/z 994.2 [M (^{174}Yb) + H]⁺. ^{31}P NMR (CD_3OD , 9.4 T, 295 K, δ): +17.7. ^{13}C NMR (CD_3OD , 296 K, 150.8 MHz, δ): 164.0 (br s, pyC⁶), 163.5 (d, pyC², $^1J = 155$ Hz), 143.9 (s, pyC⁴), 129.0 (s, pyC³), 128.1 (s, pyC⁵), 127.1 (br s, PhC²), 126.6 (d, PhC¹, $^1J = 150$ Hz), 126.3 (br s, PhC⁴), 124.0 (s, PhC³), 71.2 (s, NCH₂py), 46.8 (s, CH₂N), 36.3 (br s, CH₂N). ^1H NMR (CD_3OD , 16.5 T, 298 K, δ): 20.4 (1H, br s, pyCHN), 10.8 (9H, PhH² + pyH⁵), 10.4 (3H, s, pyH⁴), 6.80 (3H, br s, NCH'_{eq}), 5.50 (3H, s, PhH³), 4.16 (6H, s, PhH³), 0.01 (6H, br s, pyCH'N + pyH³), -2.95 (3H, br s, NCH'_{ax}), -4.73 (3H, br s, NCH_{eq}), -12.9 (3H, br s, NCH_{ax}).

[YL¹] (15 mg, 90%). Anal. Calcd for $\text{C}_{42}\text{H}_{42}\text{N}_6\text{O}_6\text{P}_3\text{Y}\cdot 3\text{H}_2\text{O}$: C, 53.5; H, 5.10; N, 8.91. Found: C, 53.2; H, 5.28; N, 8.73. ESMS⁺: m/z 908.2 [M (^{89}Y) + H]⁺. ^{31}P NMR (CD_3OD , 9.4 T, 295 K, δ): +23.9. ^1H NMR (CD_3OD , 11.7 T, 295 K, δ): 7.22 (1H, dq, $^1J_{\text{H-P}} = 536$ Hz, $^2J = 2.1$ Hz, Ph), 4.11 (2H, dq, $^2J = 36$ Hz, $^3J = 7.0$ Hz, $^3J_{\text{H-P}} = 4.0$ Hz, CH₂O), 1.54 (3H, dd, $^2J_{\text{H-P}} = 15.0$ Hz, $^3J = 2.0$ Hz, PMe), 1.23 (3H, $^3J = 7.0$ Hz, Me). ^{31}P NMR (CDCl_3 , 9.4 T, 295 K, δ): +34.5. ^{13}C NMR (CDCl_3 , 296 K, 150.8 MHz, δ): 62.3 (d, $^2J_{\text{C-P}} = 7$ Hz, CH₂O), 16.1 (Me), 14.9 (d, $^1J_{\text{C-P}} = 95$ Hz, PMe). HRMS⁺: m/z 109.0414 [M + H]⁺ ($\text{C}_3\text{H}_{10}\text{O}_2\text{P}$ requires m/z 109.0418).

Ethyl (6-Methylpyridin-2-yl)(methyl)phosphinate (4). Neat diethyl methylphosphonite (2.00 g, 14.7 mmol) was stirred at 0 °C, and H_2O (264 μL , 14.7 mmol) was added. The mixture was allowed to reach 22 °C over 1 h and stirred for a further 16 h. ^1H and ^{31}P NMR was used to confirm the formation of ethyl methylphosphinite, which was used in situ without further purification. The reaction mixture also contains 1 equiv of ethanol (>95% conversion by ^1H NMR). ^1H NMR (CDCl_3 , 11.7 T, 295 K, δ): 7.22 (1H, dq, $^1J_{\text{H-P}} = 536$ Hz, $^2J = 2.1$ Hz, Ph), 4.11 (2H, dq, $^2J = 36$ Hz, $^3J = 7.0$ Hz, $^3J_{\text{H-P}} = 4.0$ Hz, CH₂O), 1.54 (3H, dd, $^2J_{\text{H-P}} = 15.0$ Hz, $^3J = 2.0$ Hz, PMe), 1.23 (3H, $^3J = 7.0$ Hz, Me). ^{31}P NMR (CDCl_3 , 9.4 T, 295 K, δ): +34.5. ^{13}C NMR (CDCl_3 , 296 K, 150.8 MHz, δ): 62.3 (d, $^2J_{\text{C-P}} = 7$ Hz, CH₂O), 16.1 (Me), 14.9 (d, $^1J_{\text{C-P}} = 95$ Hz, PMe). HRMS⁺: m/z 109.0414 [M + H]⁺ ($\text{C}_3\text{H}_{10}\text{O}_2\text{P}$ requires m/z 109.0418).

To neat ethyl methylphosphinite, (1.59 g, 14.7 mmol), containing 1 equiv of ethanol, were added dry degassed (freeze–thaw cycle) toluene (20 mL), 2-bromo-6-methylpyridine, (2.10 g, 12.3 mmol), and triethylamine (6.0 mL, 43 mmol). Argon was bubbled through the solution for 1 h, tetrakis(triphenylphosphine)palladium(0) (320 mg, 0.27 mmol) was added, and the mixture was stirred at 125 °C for 16 h

under argon. The resulting solution was decanted from the white ammonium salt precipitate and the solvent removed under reduced pressure. Purification of the yellow oil by column chromatography on silica ($\text{CH}_2\text{Cl}_2/0\text{--}1.6\%$ CH_3OH in 0.1% increments) gave a colorless oil (700 mg, 29%). ^1H NMR (CDCl_3 , 11.7 T, 295 K, δ): 7.75 (1H, dd, $^3J = 7.0$ Hz, $^3J_{\text{H-P}} = 10$ Hz, H⁵), 7.59 (1H, td, $^3J = 7.0$ Hz, $^4J_{\text{H-P}} = 4.8$ Hz, H⁴), 7.16 (1H, d, $^3J = 7.0$ Hz, H³), 3.86 (2H, dq, $^2J = 80$ Hz, $^3J = 7.0$ Hz, H², $^3J_{\text{H-P}} = 4.5$ Hz, H⁷), 2.50 (3H, s, H¹), 1.66 (3H, d, $^2J_{\text{H-P}} = 15$ Hz, H⁹), 1.61 (3H, t, $^3J = 7.0$ Hz, H⁸). ^{13}C NMR (CDCl_3 , 296 K, 150.8 MHz, δ): 159.4 (d, $^3J_{\text{C-P}} = 20$ Hz, C²), 153.7 (d, $^1J_{\text{C-P}} = 158$ Hz, C⁶), 136.0 (d, $^3J_{\text{C-P}} = 10$ Hz, C⁴), 125.6 (d, $^2J_{\text{C-P}} = 3$ Hz, C³), 124.6 (d, $^4J_{\text{C-P}} = 22$ Hz, C⁵), 60.8 (d, $^2J_{\text{C-P}} = 6$ Hz, C⁷), 24.5 (C¹), 16.3 (C⁸) 13.3 (d, $^1J_{\text{C-P}} = 103$ Hz, H⁹). ^{31}P NMR (CDCl_3 , 9.4 T, 295 K, δ): +41.2. HRMS⁺: m/z 200.0858 [M + H]⁺ ($\text{C}_9\text{H}_{14}\text{O}_2\text{NP}$ requires m/z 200.0862). $R_f = 0.25$ (silica, $\text{CH}_2\text{Cl}_2/5\%$ MeOH).

Ethyl Methyl(6-methyl-1-oxopyridin-2-yl)phosphinate (5).

To a stirred solution of ethyl (6-methylpyridin-2-yl)(methyl)phosphinate (600 mg, 3.0 mmol) in CHCl_3 (15 mL) was added MCPBA (1.04 g, 6.0 mmol). The resulting solution was stirred at 65 °C for 16 h under argon. The reaction was monitored by TLC [silica; $\text{CH}_2\text{Cl}_2/5\%$ CH_3OH ; $R_f(\text{product}) = 0.19$; $R_f(\text{reactant}) = 0.25$] and the solvent removed under reduced pressure to give a yellow oil. CH_2Cl_2 (10 mL) was added and the solution decanted from the white precipitate. CH_2Cl_2 was removed under reduced pressure and the resultant oil purified by column chromatography on silica ($\text{CH}_2\text{Cl}_2/0\text{--}3.2\%$ CH_3OH in 0.2% increments) to give a pale-yellow oil (360 mg, 56%). ^1H NMR (CDCl_3 , 11.7 T, 295 K, δ): 7.90 (1H, dd, $^3J = 7.0$ Hz, $^3J_{\text{H-P}} = 10$ Hz, H⁵), 7.40 (1H, d, $^3J = 7.0$ Hz, H⁵), 7.26 (1H, td, $^3J = 7.0$ Hz, $^4J_{\text{H-P}} = 4.8$ Hz, H⁴), 4.03 (2H, dq, $^2J = 80$ Hz, $^3J = 7.0$ Hz, $^3J_{\text{H-P}} = 4.5$ Hz, CH₂O), 3.05 (1H, br s, OH), 2.50 (3H, s, CH₂O), 1.96 (3H, d, $^2J_{\text{H-P}} = 15$ Hz, PMe), 1.28 (3H, t, $^3J = 7.0$ Hz, Me). ^{13}C NMR (CDCl_3 , 296 K, 150.8 MHz, δ): 149.7 (d, $^3J_{\text{C-P}} = 20$ Hz, C⁶), 142.6 (d, $^1J_{\text{C-P}} = 158$ Hz, C²), 130.4 (d, $^2J_{\text{C-P}} = 3$ Hz, C⁵), 124.5 (d, $^4J_{\text{C-P}} = 22$ Hz, C³), 124.5 (d, $^3J_{\text{C-P}} = 10$ Hz, C⁴), 61.7 (d, $^2J_{\text{C-P}} = 6$ Hz, CH₂O), 17.5 (pyMe), 16.3 (CMe), 11.7 (d, $^1J_{\text{C-P}} = 103$ Hz, PMe). ^{31}P NMR (CDCl_3 , δ): +34.3. HRMS⁺: m/z 238.0607 [M + Na]⁺ ($\text{C}_9\text{H}_{14}\text{O}_2\text{NPNa}$ requires m/z 238.0609). $R_f = 0.19$ (silica, $\text{CH}_2\text{Cl}_2/5\%$ MeOH).

Ethyl [6-(Hydroxymethyl)pyridine-2-yl](methyl)phosphinate (6).

Ethyl methyl(6-methyl-1-oxopyridin-2-yl)phosphinate (360 mg, 1.67 mmol) was dissolved in CHCl_3 (10 mL), and $(\text{CF}_3\text{CO})_2\text{O}$ (8.0 mL, 56 mmol) was added. The mixture was stirred at 60 °C and the formation of the trifluoroacetate ester of the title compound monitored by LC–MS. After 3 h, the solution was cooled to 22 °C and the solvent removed under reduced pressure. The residue was dissolved in EtOH (10 mL) and the solution stirred at 60 °C for 3 h. The solvent was removed under reduced pressure to give the crude alcohol, which was purified by column chromatography (silica, $\text{CH}_2\text{Cl}_2/0\text{--}2.5\%$ CH_3OH in 0.25% increments) to give a colorless oil (220 mg, 60%). ^1H NMR (CDCl_3 , 11.7 T, 295 K, δ): 7.91 (1H, dd, $^3J = 7.0$ Hz, $^3J_{\text{H-P}} = 10$ Hz, H⁵), 7.80 (1H, td, $^3J = 7.0$ Hz, $^4J_{\text{H-P}} = 4.8$ Hz, H⁴), 7.43 (1H, d, $^3J = 7.0$ Hz, H⁵), 4.80 (2H, s, CH₂OH), 3.93 (2H, dq, $^2J = 80$ Hz, $^3J = 7.0$ Hz, $^3J_{\text{H-P}} = 4.5$ Hz, CH₂O), 1.75 (3H, d, $^2J_{\text{H-P}} = 15$ Hz, PMe), 1.24 (3H, t, $^3J = 7.0$ Hz, Me). ^{13}C NMR (CDCl_3 , 150.8 MHz, δ): 160.4 (d, $^3J_{\text{C-P}} = 20$ Hz, C⁶), 153.1 (d, $^1J_{\text{C-P}} = 156$ Hz, C²), 136.8 (d, $^3J_{\text{C-P}} = 10$ Hz, C⁴), 126.3 (d, $^4J_{\text{C-P}} = 22$ Hz, C³), 123.0 (d, $^2J_{\text{C-P}} = 4$ Hz, C⁵), 64.1 (CH₂OH), 61.1 (d, $^2J_{\text{C-P}} = 6$ Hz, CH₂O), 16.4 (Me) 13.4 (d, $^1J_{\text{C-P}} = 103$ Hz, PMe). ^{31}P NMR (CDCl_3 , δ): +40.0. HRMS⁺: m/z 216.0808 [M + H]⁺ ($\text{C}_9\text{H}_{14}\text{O}_3\text{NP}$ requires m/z 216.0801). $R_f = 0.20$ (silica, $\text{CH}_2\text{Cl}_2/7\%$ MeOH).

[6-[Ethoxy(methyl)phosphoryl]pyridine-2-yl]methyl Methanesulfonate (7).

Ethyl [6-(hydroxymethyl)pyridine-2-yl](methyl)phosphinate (110 mg, 0.51 mmol) was dissolved in anhydrous THF (3 mL), and NEt_3 (213 μL , 1.5 mmol) was added. The mixture was stirred at 5 °C, and methanesulfonyl chloride (59 μL , 0.77 mmol) was added. The reaction was monitored by TLC [silica; $\text{CH}_2\text{Cl}_2/7\%$ CH_3OH ; $R_f(\text{product}) = 0.45$; $R_f(\text{reactant}) = 0.20$] and stopped after 15 min. The solvent was removed under reduced pressure and the residue dissolved in CH_2Cl_2 (15 mL) and washed with aqueous brine (saturated, 10 mL). The aqueous layer was reextracted with CH_2Cl_2 (3

× 10 mL), the organic layers were combined and dried over MgSO₄ and the solvent was removed under reduced pressure to leave a colorless glass that was used directly in the next step without further purification (100 mg, 67%). ¹H NMR (CDCl₃, 11.7 T, 295 K, δ): 8.07 (1H, dd, ³J = 7.0 Hz, ³J_{H-P} = 10 Hz, H³), 7.92 (1H, td, ³J = 7.0 Hz, ⁴J_{H-P} = 4.8 Hz, H⁴), 7.64 (1H, d, ³J = 7.0 Hz, H⁵), 5.41 (2H, s, CH₂OS), 4.03 (2H, dqd, ²J = 80 Hz, ³J = 7.0 Hz, ³J_{H-P} = 4.5 Hz, CH₂O), 3.15 (3H, s, SMe), 1.80 (3H, d, ²J_{H-P} = 15 Hz, PMe), 1.29 (3H, t, ³J = 7.0 Hz, Me). ³¹P NMR (CDCl₃, δ): +39.4. HRMS⁺: *m/z* 294.2083 [M + H]⁺ (C₁₀H₁₀O₅NP requires *m/z* 294.2078). R_f = 0.45 (silica, CH₂Cl₂/7% MeOH).

1,4,7-Tris[ethyl-(6-methylpyridin-2-yl)(methyl)phosphinate]-1,4,7-triazacyclononane (8). 1,4,7-Triazacyclononane (15 mg, 0.12 mmol), (6-[ethoxy(methyl)phosphoryl]pyridine-2-yl)methyl methanesulfonate, 35 (100 mg, 0.34 mmol), and K₂CO₃ (47 mg, 0.34 mmol) were stirred in dry CH₃CN (4 mL) at 60 °C for 3 h under argon. The reaction was monitored by TLC to confirm consumption of the mesylate starting material. The solution was decanted from excess potassium salts and the solvent removed under reduced pressure. Purification by column chromatography on silica (CH₂Cl₂/0–20% MeOH in 1% increments) gave a colorless oil (40 mg, 47%). ¹H NMR (CDCl₃, 11.7 T, 295 K, δ): 7.89 (3H, dd, ³J = 7.0 Hz, ³J_{H-P} = 10 Hz, H³), 7.75 (3H, td, ³J = 7.0 Hz, ⁴J_{H-P} = 4.8 Hz, H⁴), 7.60 (3H, d, ³J = 7.0 Hz, H⁵), 3.95 (6H, dqd, ²J = 8 Hz, ³J = 7.0 Hz, ³J_{H-P} = 4.5 Hz, CH₂O), 3.90 (6H, br s, pyCH₂N), 2.89 (12H, br s, ring CH₂N), 1.72 (9H, d, ²J_{H-P} = 15 Hz, PMe), 1.22 (9H, t, ³J = 7.0 Hz, Me). ¹³C NMR (CDCl₃, 150.8 MHz, δ): 157.1 (d, ³J_{C-P} = 20 Hz, C⁶), 154.6 (d, ¹J_{C-P} = 156 Hz, C²), 137.1 (d, ³J_{C-P} = 10 Hz, C⁴), 126.7 (d, ⁴J_{C-P} = 20 Hz, C³), 126.2 (d, ²J_{C-P} = 4 Hz, C⁵), 64.1 (pyCH₂N), 60.9 (d, ²J_{C-P} = 6 Hz, CH₂O), 52.7 (ring CH₂N), 16.5 (Me), 13.5 (d, ¹J_{C-P} = 102 Hz, PMe). ³¹P NMR (CDCl₃, δ): +41.2. HRMS⁺: *m/z* 721.4368 [M + H]⁺ (C₃₃H₅₁O₆N₆P₃ requires *m/z* 721.4361). R_f = 0.05 (silica, CH₂Cl₂/10% MeOH).

[EuL²]. 1,4,7-Tris[ethyl (6-methylpyridin-2-yl)(methyl)phosphinate]-1,4,7-triazacyclononane (10 mg, 0.014 mmol) was dissolved in HCl (6M, 3 mL), and the solution was stirred at 100 °C for 16 h. The solvent was lyophilized to give a white solid. Hydrolysis of the ethyl groups was confirmed by ¹H and ³¹P NMR [^δ_p (CDCl₃) +34.5]. The solid was dissolved in H₂O/CH₃OH (1:1, v/v; 2 mL) and the pH of the solution adjusted to 5.8 using an aqueous NaOH solution; Eu(OAc)₃ (6.7 mg, 0.015 mmol) was added and the solution stirred at 50 °C for 18 h. After the solution was allowed to cool to room temperature, the pH was raised to 10 by the addition of an aqueous ammonia solution. The solution was stirred for 1 h, causing excess Eu³⁺ to precipitate as Eu(OH)₃, which was removed by centrifugation. Adjustment of the pH to 5.8 by the addition of acetic acid, followed by lyophilization of the solvent, gave a white solid that was purified on a short column of silica (eluting with 1% aqueous ammonia in 20% MeOH/CH₂Cl₂) to give a colorless solid (8.8 mg, 80%). Anal. Calcd for C₂₇H₃₆N₆O₆P₃Eu·4H₂O: C, 37.8; H, 5.13; N, 9.79. Found: C, 37.6; H, 5.30; N, 9.48. HRMS⁺: *m/z* 785.1127 [M + H]⁺ (C₂₇H₃₆O₆N₆P₃¹⁵¹Eu requires *m/z* 785.1121). ³¹P NMR (CD₃OD, δ): +40.1. τ(H₂O) = 1.56 ms, τ(D₂O) = 1.60 ms, and φ_{em}(H₂O) = 7.2%. UV [H₂O; λ_{max} nm (ε, M⁻¹ cm⁻¹): 272 (8400)]. ¹H NMR (CD₃OD, 9.4 T, 295 K, δ): 7.93 (3H, br s, pyH³), 7.64 (3H, br s, pyCHN), 7.39 (3H, br s, pyH⁴), 6.29 (3H, br s, pyH⁵), 4.25 (3H, br s, NCH_{eq}'), -0.40 (3H, br s, pyCH'N), -1.22 (3H, br s, NCH_{ax}'), -1.53 (3H, br s, NCH_{eq}'), -5.15 (3H, br s, NCH_{ax}').

[TbL²]. An analogous procedure was followed using 1,4,7-tris[ethyl(6-methylpyridin-2-yl)(methyl)phosphinate]-1,4,7-triazacyclononane (10 mg, 0.014 mmol) and Tb(OAc)₃ (6.2 mg, 0.015 mmol) to give a white solid (8.9 mg, 80%). ESMS⁺: *m/z* 793.1 [M (¹⁵⁹Tb) + H]⁺. HRMS⁺: *m/z* 793.1216 [M + H]⁺ (C₂₇H₃₆O₆N₆P₃¹⁵⁹Tb requires *m/z* 793.1241). ³¹P NMR (CD₃OD, δ): +5.1. τ(H₂O) = 2.59 ms, τ(D₂O) = 2.98 ms, and φ_{em}(H₂O) = 60%.

[GdL²]. An analogous procedure gave a white solid (8.6 mg, 78%). Anal. Calcd for C₂₇H₃₆N₆O₆P₃Gd·4H₂O: C, 37.6; H, 5.10; N, 9.73. Found: C, 37.8; H, 5.26; N, 9.56. ESMS⁺: *m/z* 790.1 [M (¹⁵⁶Gd) + H]⁺. r_{1p} (20 MHz, 298 K, H₂O): 1.93 mM⁻¹ s⁻¹.

A sample of the ligand 1,4,7-tri[(6-methylpyridin-2-yl)(carboxy)-1,4,7-triazacyclononane, L³, was kindly provided by Mazzanti (Grenoble) and used to allow samples of the yttrium(III) and europium(III) complexes, for purposes of comparison, using established methods described earlier.^{3b}

[YL³]. Ligand H₃L³ (15 mg, 0.028 mmol) was dissolved in H₂O (0.5 mL), and the pH of the solution adjusted to 5.8 using HCl(aq). A solution of YCl₃ (6.0 mg, 0.031 mmol) dissolved in H₂O/CH₃OH (1:1, v/v; 1 mL) was added and the solution stirred at room temperature for 16 h. The pH was raised to 10 by the addition of NaOH(aq), with the resulting precipitate of Y(OH)₃ (from excess Y³⁺) removed by centrifugation. Adjustment of the pH to 5.8 by the addition of dilute hydrochloric acid, followed by lyophilization of the solvent, gave a solid, which was purified by column chromatography (silica, CH₂Cl₂/20% CH₃OH/1% aqueous NH₄OH) to give a white solid (6.0 mg, 34%). HRMS⁺: *m/z* 643.0945 [M + Na]⁺ (C₂₇H₂₇N₆O₆Na⁸⁹Y requires *m/z* 643.0948). ¹H NMR (D₂O, 14.1 T, 295 K, δ): 8.23 (3H, t, ³J = 8 Hz, pyH⁴), 8.09 (3H, d, ³J = 8 Hz, pyH³), 7.77 (3H, d, ³J = 8 Hz, pyH⁵), 4.12 (6H, dd, pyCH₂), 3.59 (3H, br dd, H_{ax}'), 2.90 (3H, br d, H_{eq}'), 2.63 (3H, br d, H_{eq}'), 2.30 (3H, br m, H_{ax}').

[EuL³]. Ligand H₃L³ (15 mg, 0.028 mmol) was dissolved in H₂O (0.5 mL) and the pH of the solution adjusted to 5.8 using HCl(aq). A solution of EuCl₃·6H₂O (11 mg, 0.031 mmol) dissolved in H₂O (0.5 mL) was added and the solution stirred at room temperature for 16 h. The pH was raised to 10 by the addition of NaOH(aq), with the resulting precipitate of Eu(OH)₃ (from excess Eu³⁺) removed by centrifugation. Adjustment of the pH to 5.8 by the addition of HCl(aq), followed by lyophilization of the solvent, gave a solid, which was purified by column chromatography (silica, CH₂Cl₂/20% CH₃OH/1% aqueous NH₄OH) to give a white solid (11 mg, 57%). HRMS⁺: *m/z* 705.1098 [M + Na]⁺ (C₂₇H₂₇N₆O₆Na¹⁵¹Eu requires *m/z* 705.1088). ¹H NMR (D₂O, 14.1 T, 295 K, δ): 6.87 (3H, br s, pyH⁴), 6.13 (3H, br s, pyH⁵), 5.37 (3H, br s, pyCH₂), 5.07 (3H, br s, pyH³), 4.15 (3H, br s, H_{eq}'), 1.67 (3H, br s, H_{ax}'), 0.18 (3H, br s, pyCH₂), -0.25 (3H, br s, H_{eq}'), -4.71 (3H, br s, H_{ax}').

Mass Spectrometry and NMR Spectroscopy. ESMS was carried out on a Thermo Finnigan LTQ, and accurate masses were recorded on a Thermo Finnigan LTQ-FT.

¹H and ¹³C NMR spectra were recorded on Varian spectrometers operating at magnetic inductions corresponding to ¹H frequencies at 200, 400, 500, 600, and 700 MHz, e.g., Mercury 400 at 9.4 T (¹H at 399.97 MHz; ¹³C at 100.61 MHz), Mercury 200 at 4.7 T, VNMR-600 at 11.7 T, Inova 600 at 14.1 T, and VNMR-700 at 16.5 T. Spectra were recorded in commercially available deuterated solvents. All chemical shifts are given in ppm with coupling constants in Hz.

³¹P NMR longitudinal relaxation times were measured in dilute CD₃OD solutions (typically 1 mM) at 295 K using the inversion–recovery technique, without proton decoupling with chemical shifts reported relative to 85% phosphoric acid. The resulting free induction decays were subjected to backward linear prediction, optimal exponential weighting, zero-filling, Fourier transform, phasing, and baseline correction (by polynomial fitting to signal-free spectral areas). The signals were integrated by Lorentzian line fitting. An inversion–recovery-type function was fitted to the resulting data using Levenberg–Marquardt minimization of the nonlinear least-squares error functional. Each measurement was made at least three different times. A complex error analysis was performed. The experimental errors during measurement of the T₁ values were kept under 3% in each case, by ensuring a sufficient signal-to-noise ratio and a full recovery of the signal during the inversion–recovery experiment. The error associated with temperature variation was determined by measuring the relaxation rate of [TmL¹] at five temperatures over the range from 295 to 302 K. The rate R₁ varies with T⁻² (T in K) and was found to be less than 1.3% for a variation of 0.5 K. The fitting errors were determined by perturbing the relaxation rates by their standard deviations. The modified values were then used in the minimization function to determine the error quoted for the stated individual parameters.

Proton Relaxometric Studies. The water proton longitudinal relaxation rates as a function of the temperature (20 MHz) were measured with a Stellar Spinmaster FFC-2000 spectrometer (Mede, Pv, Italy) on about 0.2–0.6 mM aqueous solutions in nondeuterated water. In the case of [GdL¹], 10% methanol was added. The exact concentrations of gadolinium were determined by measurement of the bulk magnetic susceptibility shifts of a tBuOH signal on a Bruker Avance III spectrometer (11.7 T). The ¹H T₁ relaxation times were acquired by the standard inversion–recovery method with a typical 90° pulse width of 3.5 μs and 16 experiments of four scans. The reproducibility of the T₁ data was ±5%. The temperature was controlled with a Stellar VTC-91 airflow heater equipped with a calibrated copper–constantan thermocouple (uncertainty of ±0.1 °C). The proton 1/T₁ NMRD profiles were measured on a fast field-cycling Stellar SmarTracer relaxometer over a continuum of magnetic field strengths from 0.00024 to 0.25 T (corresponding to 0.01–10 MHz proton Larmor frequencies). The relaxometer operates under computer control with an absolute uncertainty in 1/T₁ of ±1%. Additional data points in the range 15–70 MHz were obtained on a Bruker WP80 NMR electromagnet adapted to VF measurements (15–80 MHz proton Larmor frequency) with a Stellar relaxometer.

ESR Spectroscopy. ESR spectra were recorded using a JEOL FA-200 ESR X-band spectrometer with a JEOL ES-LC11 flat cell for aqueous sample analysis. ESR spectroscopic analyses were carried out under the following conditions: magnetic field, 328 ± 250 mT; field modulation width, 1 mT; field modulation frequency, 100 kHz; time constant, 0.03 s; sweep time, 2 min; microwave frequency, 9.226 GHz; microwave power, 20 mW. Three scans were accumulated for each sample. The temperature of the sample was controlled with a JEOL DVT airflow heater equipped with a calibrated copper–constantan thermocouple.

Optical Spectroscopy. Emission spectra were recorded on a ISA Joblin-Yvon Spex Fluorolog-3 luminescence spectrometer. Lifetime measurements were carried out using a Perkin-Elmer LS55 spectrometer using FL Winlab software. Single-photon luminescence spectra were also recorded using an Edinburgh Instruments FLS920 Combined Fluorescence Lifetime and Steady State spectrophotometer that was equipped with a visible to near-infrared sensitive photomultiplier by a nitrogen-flow-cooled housing; LED excitation sources (365 and 465 nm) were used to excite the europium complexes. A liquid-nitrogen cryostat (77 K, Oxford Instruments) was used to cool the complexes to 77 K.

Quantum yield measurements were calculated by a comparison with two standards.³¹ For the standards and each of the unknowns, five solutions with absorbances between 0.05 and 0.1 were used. The quantum yield was calculated according to the equation

$$\Phi_x = \Phi_r \frac{A_r}{A_x} \frac{E_x}{E_r} \frac{I_r}{I_x} \frac{\eta_x^2}{\eta_r^2}$$

where r and x refer to reference and unknown, respectively; A = absorbance at λ_{ex}; E = corrected integrated emission intensity; I = corrected intensity of excitation light; η = refractive index of the solution.

HLS. The HLS technique involves the detection of an incoherently scattered harmonic generated by the irradiation of a solution of the complex with a laser of wavelength, λ.³² It leads to the measurement of the mean value of the β × β tensor product, ⟨β_{HLS}⟩. All HLS measurements were carried out in MeOH at a concentration of [LnL¹] = 1 × 10⁻³ M, and a second low-energy nonresonant incident radiation of 1.064 μm was applied. The laser line was generated by a 800 nm pump source from the fundamental femtosecond mode-locked Ti:sapphire laser system (output beam duration ~150 fs and 1 kHz repetition rate). For each complex, 10 β^{1.064} values were plotted and the Student's t distribution was employed to determine the standard deviation. The propagation of uncertainty is used to calculate the errors for the β^{1.064} values with a 95% confidence level.

X-ray Crystallography. Single-crystal X-ray data for the complexes [LnL¹] (Ln = Nd, Sm, Eu, Ho, Tm, and Yb) were reported earlier in the preliminary communication (CCDC 836097–

836102). Data for the cerium(III) complex were collected at 120 K on a Bruker SMART-CCD 6000 diffractometer (ω scan, 0.3–0.5° frame⁻¹) equipped with a Cryostream (Oxford Cryosystems) open-flow nitrogen cryostat.

Two different crystals of the cerium complex were grown by the slow evaporation of aqueous methanol, and each was examined. The first was triclinic, contained fewer solvent molecules, and was examined 2 days after crystallization; the data obtained for this crystal are reported. Another crystal was examined several weeks after crystallization and was found to be monoclinic and crystallized in the same space group as the six other lanthanide complexes reported (P2₁/n) with very similar unit cell parameters but was of lower quality and had a higher level of solvation; the data obtained were sufficient to establish the space group and confirm the chemical identity of the complex but were of lower quality and were not refined.

The structure was solved by the charge-flipping method and refined by full-matrix least squares on F² for all data using SHELXTL³³ and OLEX2³⁴ software. All nondisordered non-H atoms were refined with anisotropic displacement parameters; disordered atoms of Ph rings and P=O groups were refined isotropically with fixed SOF = 0.5. All H atoms were placed into calculated positions and refined in a “riding” mode. The structure contains a number of severely disordered solvent molecules. Their contribution to the scattering factors has been taken into account using the MASK procedure of OLEX2 software. Crystallographic data for [CeL¹] are reported in Table 1.

■ ASSOCIATED CONTENT

● Supporting Information

X-ray crystallographic files in CIF format for [CeL¹], VT EPR and VT relaxivity data for [GdL¹], comparative ¹H NMR and optical emission spectra for [EuL¹] and [EuL³]. This material is available free of charge via the Internet at <http://pubs.acs.org>.

■ AUTHOR INFORMATION

Corresponding Author

*E-mail: david.parker@dur.ac.uk.

Notes

The authors declare no competing financial interest.

■ ACKNOWLEDGMENTS

This work was supported by the European Research Council (FCC 266804), the Engineering and Physical Sciences Research Council, and CISbio Bioassays. We thank Professor M. Mazzanti (Grenoble) for a sample of L³ and dedicate this paper to Herve le Bozec in Rennes.

■ REFERENCES

- (1) (a) Montgomery, C. P.; Murray, B. S.; New, E. J.; Pal, R.; Parker, D. *Acc. Chem. Res.* **2009**, *42*, 925. (b) Zucchi, G.; Jeon, T.; Tondelier, D.; Aldakov, D.; Thuery, P.; Ephritikhine, M.; Geffroy, B. *J. Mater. Chem.* **2010**, *20*, 2114. (c) Moore, E. G.; Samuel, A. P. S.; Raymond, K. N. *Acc. Chem. Res.* **2009**, *42*, 542. (d) Eliseeva, S. V.; Bunzli, J.-C. G. *Chem. Soc. Rev.* **2010**, *39*, 189.
- (2) (a) Ryan, P. E.; Guenee, L.; Canard, G.; Gummy, F.; Bunzli, J.-C. G.; Piguet, C. *Inorg. Chem.* **2009**, *48*, 2549. (b) Renaud, F.; Piguet, C.; Bernardinelli, G.; Bunzli, J.-C. G.; Hopfgartner, G. *J. Am. Chem. Soc.* **1999**, *121*, 9326. (c) Koeller, S.; Bernardinelli, G.; Piguet, C. *Dalton Trans.* **2003**, 2395. (d) Picot, A.; D'Aleo, A.; Baldeck, P. L.; Grichine, A.; Duperray, A.; Andraud, C.; Maury, O. *J. Am. Chem. Soc.* **2008**, *130*, 1532.
- (3) (a) Charbonniere, L.; Ziessel, R.; Guardigli, M.; Roda, A.; Sabbatini, N.; Cesario, M. *J. Am. Chem. Soc.* **2001**, *123*, 2436. (b) Gateau, C.; Mazzanti, M.; Pecaut, J.; Dunand, F. A.; Helm, L. *Dalton Trans.* **2003**, 2428. Nocton, G.; Nonat, A.; Gateau, C.; Mazzanti, M. *Helv. Chem. Acta* **2009**, *92*, 2257. Giraud, M.; Andreiadis, E. S.; Fisyuk, A. S.; Demadrille, A.; Pecaut, J.; Imbert, D.; Mazzanti, M.

- Inorg. Chem.* **2008**, *47*, 3952. Nonat, A.; Giraud, M.; Gateau, C.; Fries, P. H.; Helm, L.; Mazzanti, M. *Dalton Trans.* **2009**, 8033. Nonat, A.; Gateau, C.; Fries, P. H.; Mazzanti, M. *Chem.—Eur. J.* **2006**, *12*, 7133. (c) Hovinen, J.; Guy, P. M. *Bioconjugate Chem.* **2009**, *20*, 404. Takalo, H.; Hemmila, I.; Sutela, T.; Latva, M. *Helv. Chim. Acta* **1996**, *79*, 789. (d) Tei, L.; Baum, G.; Blake, A. J.; Fenske, D.; Schroder, M. *J. Chem. Soc., Dalton Trans.* **2000**, 2793. (e) Tei, L.; Blake, A. J.; Wilson, C.; Schroder, M. *J. Chem. Soc., Dalton Trans.* **2004**, 1945. (f) Murphy, B. P.; Quinti, L.; Kelly, D. G.; Martin, W. J.; Perotti, A.; Hursthouse, M. B.; Gelbrich, T. *Inorg. Chem. Commun.* **2002**, *5*, 577.
- (4) (a) Aime, S.; Batsanov, A. S.; Botta, M.; Howard, J. A. K.; Parker, D.; Senanayake, K.; Williams, G. *Inorg. Chem.* **1994**, *33*, 4696. (b) Huskens, J.; Sherry, A. D. *J. Chem. Soc., Dalton Trans.* **1998**, 177. (c) Broan, C. J.; Cole, E.; Jankowski, K. J.; Parker, D.; Pulukoddy, K.; Boyce, B. A.; Beeley, N. R. A.; Millar, K.; Millican, A. T. *Synthesis* **1992**, *13*, 63. (d) Chalmers, K. H.; Botta, M.; Parker, D. *Dalton Trans.* **2011**, 40, 904. (e) Vitha, T.; Kubicek, V.; Kotek, J.; Hermann, P.; Van der Elst, L.; Muller, R. N.; Lukes, I.; Peters, J. A. *Dalton Trans.* **2009**, 3204. (f) Forsterova, M.; Svobodova, J.; Lubal, P.; Taborsky, P.; Kotek, J.; Hermann, P.; Lukes, I. *Dalton Trans.* **2007**, 535.
- (5) (a) Notni, J.; Hermann, P.; Havlickova, J.; Kotek, J.; Kubicek, V.; Plutnar, J.; Loktionova, N.; Riss, P. J.; Rosch, F.; Lukes, I. *Chem.—Eur. J.* **2010**, *16*, 7174. (b) Cole, E.; Copley, R. C. B.; Howard, J. A. K.; Parker, D.; Ferguson, G.; Gallagher, J. F.; Kaitner, B.; Harrison, A.; Royle, L. *J. Chem. Soc., Dalton Trans.* **1994**, 1619.
- (6) Walton, J. W.; Di Bari, L.; Parker, D.; Pescitelli, G.; Puschmann, H.; Yufit, D. S. *Chem. Commun.* **2011**, 47, 12289.
- (7) (a) Tancrez, N.; Feuvrie, C.; Ledoux, I.; Zyss, J.; Toupet, L.; Le Bozec, H.; Maury, O. *J. Am. Chem. Soc.* **2005**, *127*, 13474. (b) Furet, E.; Costuas, K.; Rabiller, P.; Maury, O. *J. Am. Chem. Soc.* **2008**, *130*, 2180. (c) Maury, O.; Le Bozec, H. *Acc. Chem. Res.* **2005**, *38*, 691. (d) Senecal-david, K.; Hemercyck, A.; Tancrez, N.; Toupet, L.; Williams, J. A. G.; Ledoux, I.; Zyss, J.; Boucekkine, A.; Guegan, J.-P.; Le Bozec, H.; Maury, O. *J. Am. Chem. Soc.* **2006**, *128*, 12243.
- (8) Valore, A.; Cariati, E.; Righetto, S.; Roberto, D.; Tessore, F.; Ugo, R.; Fragala, I. L.; Fragala, M. E.; Malandrino, G.; De Angelis, F.; Belpassi, L.; Ledoux-Rak, I.; Thi, K. H.; Zyss, J. *J. Am. Chem. Soc.* **2010**, *132*, 4966.
- (9) Law, G.-L.; Wong, K.-L.; Lau, K.-K.; Lap, S.; Tanner, P. A.; Kuo, F.; Wong, W.-T. *J. Mater. Chem.* **2010**, *20*, 4074.
- (10) Bogani, L.; Cavigli, L.; Bernot, K.; Sessoli, R.; Gurioli, M.; Gatteschi, D. *J. Mater. Chem.* **2006**, *16*, 2587.
- (11) Boekelheide, V.; Linn, W. J. *J. Am. Chem. Soc.* **1954**, *76*, 1286.
- (12) Shannon, R. D. *Acta Crystallogr., Sect. A* **1976**, *32*, 751.
- (13) Aime, S.; Batsanov, A. S.; Botta, M.; Dickins, R. S.; Faulkner, S.; Foster, C. E.; Harrison, A.; Howard, J. A. K.; Moloney, J. M.; Norman, T. J.; Parker, D.; Royle, L.; Williams, J. A. G. *J. Chem. Soc., Dalton Trans.* **1997**, 3623.
- (14) Aime, S.; Barbero, L.; Botta, M.; Ermondi, G. *J. Chem. Soc., Dalton Trans.* **1992**, 225.
- (15) (a) Bleaney, B. *J. Magn. Reson.* **1972**, *8*, 91. (b) Peters, J. A.; Huskens, J.; Raber, D. *J. Prog. Nucl. Magn. Reson. Spectrosc.* **1996**, *28*, 283. (c) Campello, M. P. C.; Lacerda, S.; Santos, I. C.; Pereira, G. A.; Geraldes, C. F. G. C.; Kotek, J.; Hermann, P.; Vanek, P.; Lubal, P.; Kubicek, L.; Toth, E.; Santos, I. *Chem.—Eur. J.* **2010**, *16*, 8446.
- (16) Parker, D.; Dickins, R. S.; Puschmann, H.; Crossland, C.; Howard, J. A. K. *Chem. Rev.* **2002**, *102*, 1977.
- (17) (a) Freed, J. H. *J. Chem. Phys.* **1978**, *68*, 4034. (b) Polnaszek, C. F.; Bryant, R. G. *J. Chem. Phys.* **1984**, *81*, 4038. (c) Bloembergen, N.; Morgan, L. O. *J. Chem. Phys.* **1961**, *34*, 842. (d) Bertini, I.; Luchinat, C.; Parigi, G. *Adv. Inorg. Chem.* **2005**, *57*, 105. (e) Helm, L. *Prog. NMR Spectrosc.* **2006**, *49*, 45.
- (18) (a) Caravan, P.; Ellison, J. J.; McMurry, T. J.; Lauffer, R. B. *Chem. Rev.* **1999**, *99*, 2293. (b) Reuben, J. *J. Phys. Chem.* **1971**, *75*, 3164. (c) Powell, D. H.; Merbach, A. E.; Gonzalez, G.; Brucher, E.; Micshei, K.; Ottaviciu, M. F.; Kohler, K.; Von Zelewsky, A.; Grintuz, O. Y.; Lebedev, Y. S. *Helv. Chim. Acta* **1993**, *76*, 2129.
- (19) (a) Bertini, I.; Capozzi, F.; Luchinat, C.; Nicastro, G.; Xia, Z. *J. Phys. Chem.* **1993**, *97*, 6351. (b) Finn, C. B. P.; Orbach, R.; Wolf, W. P. *Proc. Phys. Soc. (London)* **1961**, *77*, 261. (c) Orbach, R. *Proc. Phys. Soc. (London)* **1961**, *A77*, 821. (d) Jensen, M. R.; Led, J. J. *J. Magn. Reson.* **2004**, *167*, 169. (e) Fries, P.; Gateau, C.; Mazzanti, M. *J. Am. Chem. Soc.* **2005**, *127*, 15801.
- (20) (a) Dickins, R. S.; Bruce, J. I.; Parker, D.; Tozer, D. *J. Dalton Trans.* **2003**, 1264. (b) Nonat, A.; Imbert, D.; Pecaut, J.; Giraud, M.; Mazzanti, M. *Inorg. Chem.* **2009**, *48*, 4207. (c) Balogh, E.; Mato-Iglesias, M.; Platas-Iglesias, C.; Toth, E.; Djanashvili, K.; Peters, J. A.; de Blas, A.; Rodrigues-Blas, T. *Inorg. Chem.* **2006**, *45*, 8719. (d) Bonnet, C. S.; Fries, P. H.; Gabelle, A.; Gambaelli, S.; Delange, P. *J. Am. Chem. Soc.* **2008**, *130*, 10401. (e) Belorizky, E.; Fries, P. H.; Helm, L.; Kowalewski, J.; Kruk, D.; Sharp, R. R.; Westlund, P. O. *J. Chem. Phys.* **2008**, *128*, 052315. (f) Borel, A.; Kang, H.; Gateau, C.; Mazzanti, M.; Clarkson, R. B.; Belford, R. L. *J. Phys. Chem. A* **2006**, *110*, 12434.
- (21) Chalmers, K. H.; De Luca, E.; Hogg, N. H. M.; Kenwright, A. M.; Kuprov, I.; Parker, D.; Botta, M.; Wilson, J. I.; Blamire, A. M. *Chem.—Eur. J.* **2010**, *16*, 134.
- (22) Gueron, M. *J. Magn. Reson.* **1975**, *19*, 58.
- (23) Alsaadi, B. M.; Rossotti, F. J. C.; Williams, R. J. P. *J. Chem. Soc., Dalton Trans.* **1980**, 2151.
- (24) (a) Bertini, I.; Capozzi, F.; Luchinat, C.; Nicastro, G.; Xia, G. *J. Phys. Chem.* **1993**, *97*, 6351. (b) Gignoux, D.; Schmitt, D.; Zeguine, M. *J. Magn. Magn. Mater.* **1987**, *66*, 373. (c) Chevalier, B.; Tence, S.; Andre, G.; Matier, S. F.; Gaudin, E. *J. Phys. Conf. Ser.* **2010**, *200*, 032012. (d) Jensen, J.; Mackintosh, A. K. *Rare Earth Magnetism*; Clarendon Press: Oxford, U.K., 1991.
- (25) (a) Beeby, A.; Clarkson, I. M.; Dickins, R. S.; Faulkner, S.; Parker, D.; Royle, L.; de Sousa, A. S.; Williams, J. A. G.; Woods, M. *J. Chem. Soc. Perkin Trans. 2* **1999**, 493. (b) Dickins, R. S.; Parker, D.; de Sousa, A. S.; Williams, J. A. G. *Chem. Commun.* **1996**, 697.
- (26) Petoud, S.; Muller, G.; Moore, E. G.; Xu, J.; Sokolnicki, J.; Riehl, J. P.; Le, U. N.; Cohen, S. M.; Raymond, K. N. *J. Am. Chem. Soc.* **2007**, *129*, 77.
- (27) Forster, D. R.; Richardson, F. S. *Inorg. Chem.* **1983**, *22*, 3996.
- (28) Kang, J.-G.; Kim, T.-J. *Bull. Korean Chem. Soc.* **2005**, *26*, 1057.
- (29) Mason, S. F.; Peacock, R. D.; Stewart, B. *Mol. Phys.* **1975**, *30*, 1829.
- (30) Mason, S. F. *Struct. Bonding (Berlin)* **1980**, *39*, 43. Reid, M. F.; Richardson, F. S. *Chem. Phys. Lett.* **1983**, *95*, 5012.
- (31) Walton, J. W.; Lamarque, L.; Parker, D.; Zwier, J. *Eur. J. Inorg. Chem.* **2010**, 25, 3961.
- (32) (a) Maker, P. D. *Phys. Rev. A* **1970**, *1*, 923. (b) Clays, K.; Persoons, A. *Phys. Rev. Lett.* **1991**, *66*, 2980. (c) Zyss, J.; Ledoux, I. *Chem. Rev.* **1994**, *94*, 77. (d) Brasselet, S.; Zyss, J. *J. Opt. Soc. Am. B* **1998**, *15*, 257. (e) Eienthal, K. B. *Chem. Rev.* **1996**, *96*, 1343. (f) Kaatz, P.; Shelton, D. P. *J. Chem. Phys.* **1996**, *105*, 3918.
- (33) Sheldrick, G. M. *Acta Crystallogr., Sect. A* **2008**, *64*, 112.
- (34) Dolomanov, O. V.; Bourhis, L. J.; Gildea, R. J.; Howard, J. A. K.; Puschmann, H. *J. Appl. Crystallogr.* **2009**, *42*, 339.